Winter 12-1-2012

Development & Testing of Novel Atmospheric Chemistry Technologies

Peter Johnson Mellott
Washington University in St. Louis

WASHINGTON UNIVERSITY IN ST. LOUIS

School of Engineering and Applied Science

Department of Energy, Environmental & Chemical Engineering

Thesis Examination Committee:
Brent Williams, Chair
Pratim Biswas
Da-Ren Chen

DEVELOPMENT & TESTING OF NOVEL ATMOSPHERIC CHEMISTRY TECHNOLOGIES

by

Peter Johnson Mellott

A thesis presented to the School of Engineering
of Washington University in partial fulfillment of the
requirements for the degree of

MASTER OF SCIENCE

December 2012
Saint Louis, Missouri

ABSTRACT OF THE THESIS

Development & Testing of Novel Atmospheric Chemistry Technologies

by

Peter Mellott

Master of Science in Energy, Environmental & Chemical Engineering

Washington University in St. Louis, 2012

Research Advisor: Professor Brent Williams

Atmospheric aerosols play an important role in global atmospheric chemistry and climate and have a detrimental impact on human health. Advancements in measurement technologies allow for better monitoring of atmospheric composition and dynamics, creating better predictive models and understanding of atmospheric chemistry and physics. Gas and particle atmospheric oxidation is poorly understood. In order to create a better understanding of atmospheric oxidation, the following equipment was developed: 1) a Potential Aerosol Mass (PAM) flow reaction chamber was developed to create reproducible steady-state oxidation of organic species in a controlled laboratory setting, 2) a custom combustion chamber for introduction of realistic single source samples, and 3) a Thermal desorption Aerosol Gas chromatograph (TAG) for hourly speciation of hundreds of semi-volatile and non-volatile organic compounds. Development and construction of the Combustion Chamber, PAM Chamber, and TAG system are discussed as well as preliminary applications of this equipment. These instruments allow for the study of primary organic aerosol (POA) and secondary organic aerosol (SOA) formation. Due to the lack of knowledge concerning organic aerosol source chemical profiles and subsequent chemical

evolution in the atmosphere, these studies are crucial for furthering the understanding of atmospheric chemistry and in developing accurate atmospheric models.

Acknowledgments

I would like to thank everyone who helped with this project: Steve Picker for his help with the construction of the electronic controls, Chris Ruehl for taking the time to help with the Labview programing, Prof. William Brune and his group for their help with the PAM chamber, John Jayne for his design of the Denuder End Caps, my labmates for all of their help putting this together. Specifically, Dhruv Mitroo, Raul Martinez, Neil Feinberg, Craig Jacobson, Andrew Spitz, Samantha Rosenthal and William Swanson for their specific contributions. I would like to thank Prof. Jay Turner for the experience working in his laboratory.

I would also like to thank to my advisor, Prof. Brent Williams, for all his help with making this thesis happen.

Thank you to my committee members, Prof. Pratim Biswas, and Prof. Da-Ren Chen.

Thank you to International Center for Advanced Renewable Energy and Sustainability (ICares) and Washington University for funding this research.

Finally, I would like to thank all my friends and family for supporting me during my work here.

Peter Mellott

Contents

List of Tables

List of Figures

Chapter 1

Introduction and Motivation

Due to adverse impacts on climate and human health [1], continued advancement towards a better understating of global atmospheric chemistry is critical. Atmospheric composition measurements are helping to identify pollution sources and various chemical pathways. Examples of impacts upon human health include cardiovascular and respiratory problems. According to the 2007 IPCC report [1], in terms of global radiative forcing mechanisms, particulates are the least understood, with the highest uncertainty of impact. Particulates provides the largest errors in current climate change models.[1] As can be seen in Fig 1.1, greenhouse gases (GHG) have a net warming effect, while aerosols have a net cooling effect. However, unlike the GHGs, aerosols have large errors associated with them. In addition, organics make up a large mass fraction of atmospheric aerosols, up to 90% of the submicron particulates[2]. Although primary aerosols and inorganic species have been fairly well characterized over the years, there is a lack of knowledge concerning secondary organic aerosol (SOA) formation and oxidization pathways. SOA from biogenic sources can make up to 90% of the SOA in the atmosphere [3]. Volatile organic compounds (VOC) complete oxidation eventually results in CO2. However, not all species are completely oxidized, as there are many different fragmentation, functionalization, and oligomerization reactions that can take place [6]. This complexity makes it challenging to predict the amount of SOA formation in the atmosphere using current models[18]. Secondary aerosol formation pathways and oxidized emission profiles are poorly understood. SOA forms when hydroxyl radicals, ozone, or nighttime nitrate radicals react with volatile organic compounds to form lower volatility reaction products [31]. Current models predict only a small fraction of the organic aerosols. This underestimation ranges by a factor 4 to 100 [4]. Therefore, novel laboratory and experimental instrumentation and techniques are required to further study SOA formation and oxidation pathways.

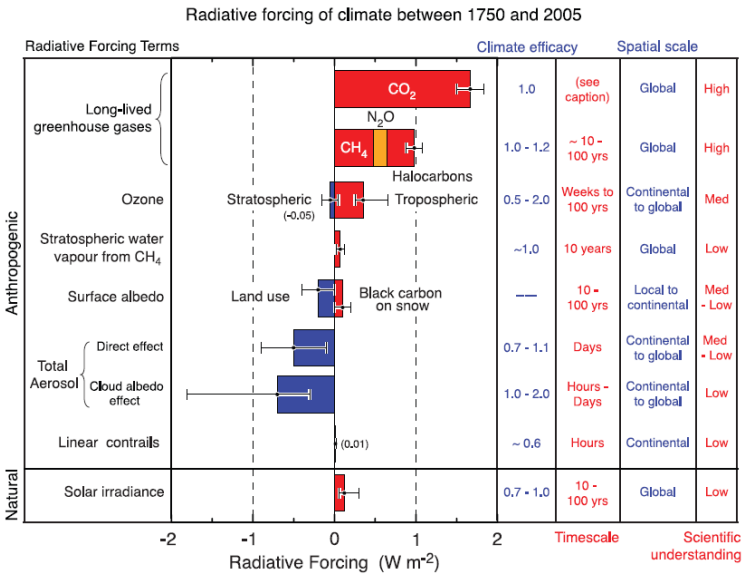

Figure 1.1 Radiative Forcing of Climate Between 1750 and 2005 [1]

Understanding atmospheric chemistry and advancements in modeling of SOA has therefore become an area of significant interest. With the uncertainty of SOA formation in current models, it is important to understand the chemical pathways of organic aging and SOA formation. α-Pinene is a very common volatile organic species in the atmosphere, accounting for a significant portion of biogenic VOC emissions to the atmosphere, with estimated emissions around 50 Tg of Carbon per year [5]. Being fairly well studied in terms of its oxidation pathways and resulting SOA formation, α-pinene can be used as a reference species.

In order to answer remaining questions on organic aerosol sources and transformation processes, new instrumentation and experimental methods must be developed. Previous technologies either do not have high time resolution or are lacking the speciation necessary to understand SOA formation mechanisms. Thermal Desorption Aerosol GC/MS (TAG) [19] was recently developed to offer a way to measure particle composition with both high chemical speciation and 1-hour time resolution. Combining this with the recently developed Potential Aerosol Mass (PAM) chamber [16] allows laboratory simulations of atmospheric aging of species and a method to rapidly measure the products. By oxidizing α-pinene in the PAM chamber, it is possible to determine the sensitivity of the TAG to previously reported α-pinene oxidation products and to rapidly determine chemical composition changes over a wide range of oxidant exposure, mimicking the atmospheric

aging process. Using a well-studied species such as α-pinene allows us to test the ability of the PAM chamber to produce an oxidizing environment similar to prior Teflon smog chambers [14] and that is relevant for atmospheric conditions.

Chapter 2

Background

2.1 Primary and Secondary Organic Aerosols and Oxidation of Species

Atmospheric composition has been monitored at many locations, primarily in the Northern Hemisphere [16]. Rogge et al. published a series of chemical profiles for various emissions such as burning leaves, tires, asphalt roofing and many other samples[21][22][23]. These source profiles are very useful when identifying material collected near the emission source. However, Rogge et al. did not consider the atmospheric aging of the samples when creating the chemical profiles. At varying rates, most organics in the atmosphere will experience oxidation, transforming original chemical profiles. In addition, a large portion of emissions are in the gas phase. Atmospheric oxidation causes these molecules to form secondary particle mass, SOA. Globally, a majority of fine particle organic matter is secondary in nature [24]. As a result, it is difficult to use these primary chemical profiles to identify sources in the atmosphere without knowledge of SOA chemical profiles. Kroll et al. (2011) illustrate how atmospheric oxidation causes organics to move towards a final product of CO_2(see figure 2.1)[6].

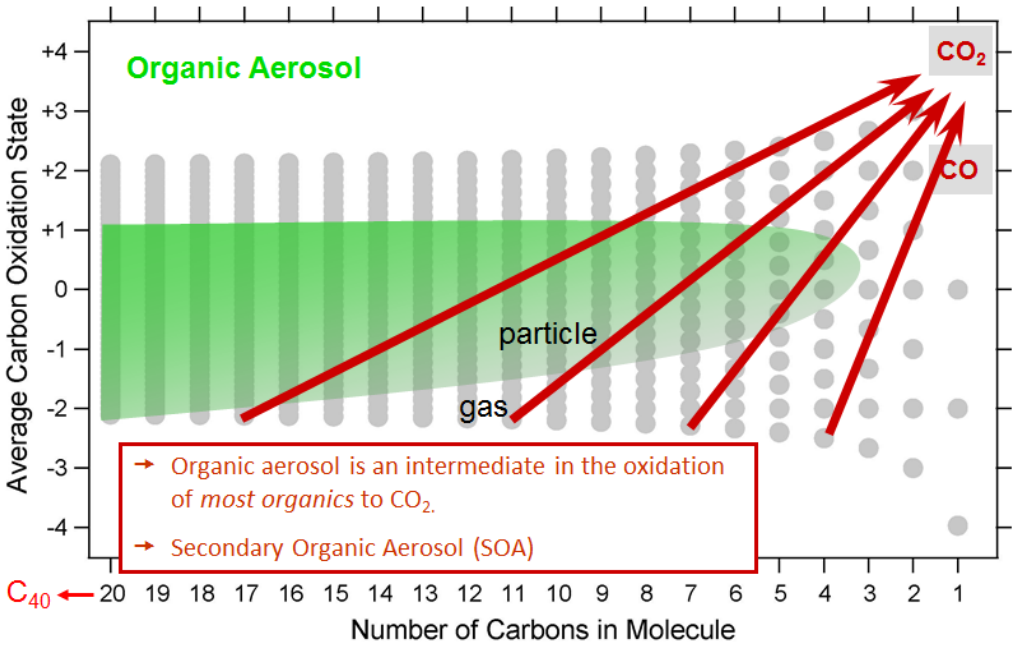

Figure 2.1 Oxidation Trends of Organics, [6]

This type of oxidation is critical because along these oxidation pathways, material that started as volatile organic species can transform to non-volatile species and form SOA. These pathways allow a small number of primary species to create a large number of secondary organics [7]. With further oxidation these species eventually tend towards CO_2. However, once they are in the particle phase, there are many other pathways for the particle removal including settling, rainout, and interception.

2.2 α-Pinene Oxidation: An Example System

In order to test the performance of the TAG system and PAM chamber, we first look at the established oxidation mechanism of a known species. For this we use α-pinene. α-Pinene is used as a standard for oxidation mechanisms. Laboratory measured oxidation pathways for α-pinene have been studied, and models exist that can be used as a predictive tool to better understand the operation of the TAG system and PAM chamber [8][9][10].

α-Pinene is a bi-cyclic carbon molecule with 10 carbons featuring a double bond. There are multiple potential oxidation and reaction pathways and a large number of potential

products. α-Pinene is highly reactive with OH and O_3, therefore the majority of the degradation involves reaction with these species. Valorso [8], Capouet [9], and Noziere [10] present potential systems of reactions in the oxidation of α-pinene. In addition to the potential pathways, the kinetics driving the α-pinene reactions must be understood in order to predict the resulting composition at various stages of the oxidation process. Models for simulating α-pinene are presented here and compared with results from laboratory experiments determining α-pinene derived products and pathways.

Detailed simulations of α-Pinene reactions have been conducted by Valorso et al. using GECKO-A (Generator for Explicit Chemistry and Kinetics of Organics in Atmosphere)[8]. They present potential reaction pathways for these different species. GECKO-A is a tool for creating chemical pathway models. Conventional models apply data from laboratory smog chamber oxidation experiments. However, given the previously mentioned deficiencies of atmospheric measurement technologies, this does not necessarily reveal the correct pathways in the reaction, only the end results. GECKO-A can be used to self-generate the pathways by which these reactions take place. SOA formation chemical dynamics can be described by the model. The GECKO-A model used by Valorso et al. constrained the model in order to allow computation to be practical. This is important because, for example, there are approximately one million chemicals in an explicit model for octene. In order to make the model practical to use, limiting the number of the product species is crucial. A million chemical species is approaching the limit of what is currently computationally possible. In order to model structures with more carbon atoms, protocols are implemented with GECKO-A to create limits on the processing. These include removing non-volatile species from the model and isomer substitution. Removal of non-volatiles is logical because non-volatile species will not participate in the gaseous reactions of the system.

Below are the OH oxidation pathways as determined by GECKO-A by Valorso et. al.[8] Shown are the initial pathways and products of the oxidation of α-pinene initiate by the hydroxyl radical. The final products and many intermediate products are not listed here, and only the first few steps in the oxidation pathway are shown. The products shown below continue to oxidize until they either form non-volatile species or oxidize to CO and CO_2[8].

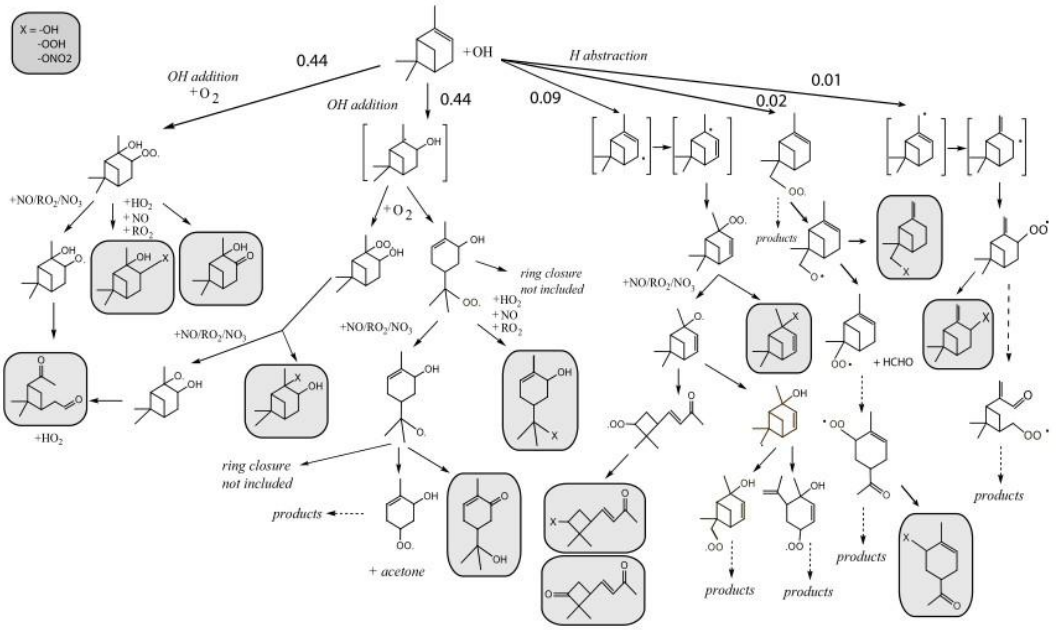

Figure 2.2 Oxidation Pathways and Yields for α-Pinene, [8]

Other studies of α-pinene oxidation can be compared with Valorso et al.[8] Capouet et al.[9] studied α-pinene OH oxidation, creating a detailed reaction mechanism and analyzing the resulting mechanism against laboratory results from Noziere et al. [9][10]. From 30 experiments, time profiles of species were taken in order to validate the model by Capouet et al.[9]. The Capouet et al.[9] model is a near-explicit model for α-pinene and pinonaldehyde OH oxidation. Similar to the mechanism by Valorso et al.[8], Capouet et al.[9] encountered the challenging issue of having a large chemical space. In order to address this issue, Capouet et al. [9] implemented a few techniques.

Species can be divided into 3 volatility bins. The first is made up of the non-volatile species, defined by having a vapor pressure less than 10^{-13} atm. The middle bin is then comprises species with vapor pressures between 10^{-13} and 10^{-5} atm. The most volatile bin consists of species with volatilities above 10^{-5} atm. Species in the lowest volatility bin tend to settle or condense and will not participate in the oxidation chemistry, allowing predictive models to view these species as a sink[8]. In order to create the protocol for removing low vapor pressure species, the vapor pressures of all the species must be known first. Structure Activity Relationships (SARs) are used to estimate vapor pressures for SOA formation.

Jimenez et al. [24] illustrate the progression through these volatility bins. During oxidation, species can start in the volatile phase, move into the semi-volatile oxygenated

organic aerosol phase, and then finally into the low volatility volatile oxygenated organic aerosol phase. This is show in Fig. 2.3.

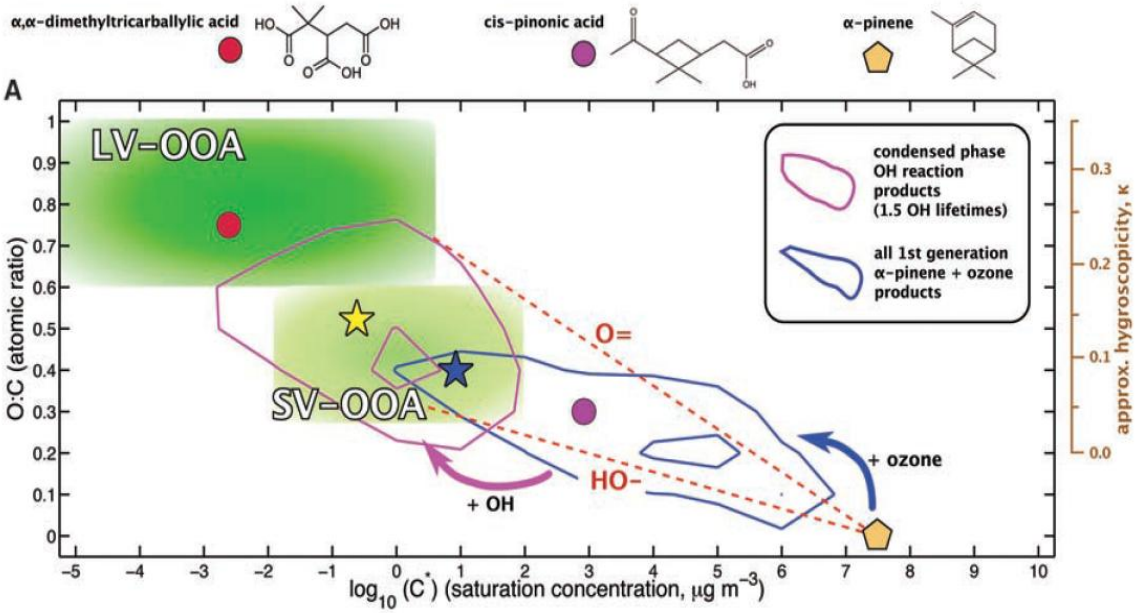

Figure 2.3 Illustrating Volatility Bins with α-Pinene Oxidation, [24]

SARs were implemented by Capouet et al.[9], as well as density functional theory for barrier heights and statistical rate theories to generate this model. This model provided the main degradation pathways of α-pinene OH addition and H-abstraction. OH addition accounts for 88% of α-pinene degradation through two pathways, roughly evenly split, while H-abstraction makes up the additional 12% [9]. The full oxidation pathway proposed by Capouet et al.[9] can be seen in the Appendix A.

When Capouet et al.[9] compared the theoretical mechanism with Valorso et al[8], the two mechanisms were identical. Using laboratory data from Noziere et al.[10], the mechanisms are in good agreement. All major chemical pathways follow the same routes. This is expected, both studies use similar modeling methods. Therefore, verification by laboratory studies is important. However, detailed degradation mechanisms on many of the secondary products have not been conducted in laboratories due to the very large number of species and the difficulty (eg. wall interactions) of performing longer oxidation experiments (achieving a higher oxidation state) within static Teflon smog chambers. Because of this, for many of the secondary products, it is necessary to assume the degradation will follow paths similar to those determined by the explicit mechanism.

Validation of the models by experimentation is critical. The Noziere laboratory studies measure α-pinene oxidation yields, pathways and products[10]. Unlike most previous studies, the secondary oxidation mechanisms were measured in addition to the primary α-pinene oxidation. With OH being the predominant oxidation mechanism, mercury lamps generated OH via H_2O_2 and CH_3ONO photolysis:

$$H_2O_2 + h\nu \rightarrow 2\ OH \qquad h\nu = 253.7\ nm$$

$$CH_3ONO + h\nu \rightarrow CH_3O + NO \qquad h\nu = 360\ nm$$

$$CH_3O + O_2 \rightarrow CH_2O + HO_2$$

$$NO + HO_2 \rightarrow NO_2 + OH$$

In the case of CH_3ONO photolysis, it is important to note whether the experiment takes place in a high NOx or low NOx environment. Noziere et al.[10] created a system similar to atmospheric conditions by using a TL-05 lamp which radiates primarily in the 300-480 nm range [10]. Noziere et al.[10] used a 1080 l quartz reactor and infrared spectroscopy to age and measure the reactants and products of the system. The experiment used both systems with and without NOx allowing the CH_3ONO precursor to OH to be photolyzed in some experiments while in others only the H_2O_2 source was active. This variety allows determination of the various OH-source kinetics. Formation of aerosols was monitored with an SMPS with a 4 minute time resolution. The system monitored size distribution in order to determine the fractional yield of the α-pinene conversion to aerosol. Full experimental details can be found in Noziere et al 1999.[10]

Unlike the explicit models, the mechanisms for oxidation by Noziere et al. do not easily determine intermediate species due to the rapid reaction of the species. The primary product of α-pinene oxidation is pinonaldehyde. The relative yield was corrected to account for OH reactions with the pinonaldehyde. This is done in conjunction with the experimental measurements of the pinonaldehyde oxidation mechanism as an internal mechanism to the α-pinene oxidation. Other major products of α-pinene reaction in the presence of NOx include nitrates, formaldehyde, and acetone. In the absence of NOx, the nitrates are not present. The yields for the various species of α-pinene oxidation are given below.

Table 2.1 Oxidation Yields from α-Pinene, [10]

	Pinonaldehyde	Total Nitrates	Formaldehyde	Acetone
NOx present	87±20%	18±9%	23±9%	9±6%
No NOx	37±7%		8±1%	7±2%

The pathways that Noziere et al.[10] proposes are shown below. Noziere et al.[10] quantifies the yields of the various products of the pathways.

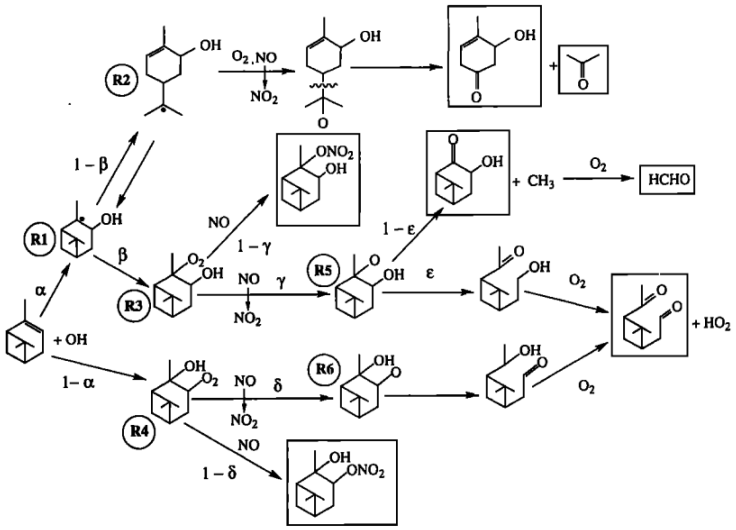

Figure 2.4 Oxidation Pathways α-Pinene with NOx, [10]

A comparison of systems with NOx and systems without NOx illustrates important characteristics of the oxidation of α-pinene. In the above diagram, α stands for regioselectivity of OH addition, β represents the competition between R1 reacting with O_2 or isomerizing into R2. γ, δ represent the branching ratio of reactions with NO and the formation of alkylnitrates, and ε are branching ratio of the R5 ring opening to decomposing to formaldehyde [10]. Noziere et al.[10] solves for the following values based upon the yields of acetone, formaldehyde, overall nitrate, and pinonaldehyde. α=0.65, β=0.90 γ=0.925 δ=0.75 ε=0.69. The full system of equations is shown in the Appendix B.

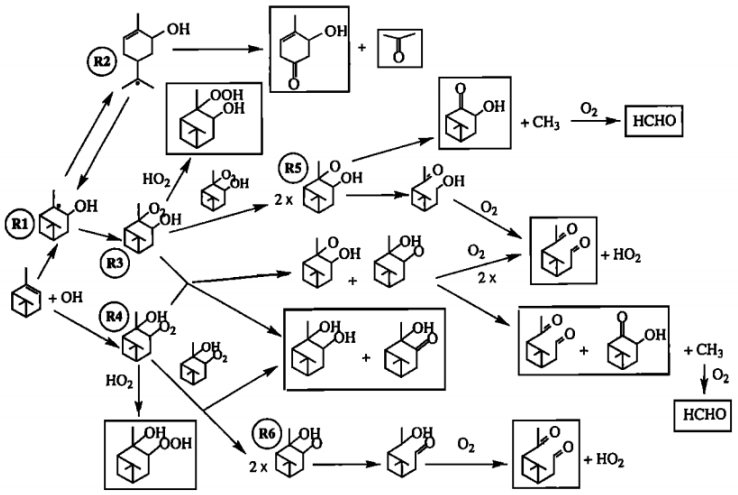

Figure 2.5 Oxidation Pathways α-Pinene without NOx, [10]

Most of the species occurring with NOx are present without NOx. However, the oxidation mechanism is more complex in the case without NOx. This is due to R3 and R4 seen in Figure 2.4. These peroxy radicals can either react with each other or with HO_2. This complexity makes it difficult to characterize the creation of R5 and R6.

Having shown that models can predict pathways and kinetics for oxidation mechanisms, secondary organic aerosol (SOA) formation from α-pinene, Pathak et al.[12] looked at the ozonolysis of α-pinene with respect to quantitative SOA formation. The SOA yields depend upon α-pinene, OH and O_3 concentrations and temperature. Aerosol Mass Fraction (AMF) is the mass of SOA formed divided by the mass of reacted α-pinene [12]. Smog chambers were used to study the effect of varying conditions. As α-pinene concentrations increase, so does the AMF. This occurs rapidly at low α-pinene concentrations and slows as α-pinene increases. When either NOx or UV lights were present, AMF decreased. In the presence of water, SOA formation was reduced. Weak temperature dependency was observed from 15 to 40°C. However, AMF decreases by a factor of 2 when temperature increased from 0 to 15°C. Pathak et al.[12] also found that seed aerosol, while not having an effect on the final AMF for chamber studies, are crucial for reducing error for inline aging studies. Rapid nucleation and generation nucleation sites cause the addition of aerosol seeds to have a diminished effect[12]. As can be seen below, as α-pinene oxidizes, a large amount of SOA is formed. If the 50 Tg/yr were all reacted, α-

pinene oxidation would account for somewhere between 1 and 10 Tg of SOA per year according to these results.

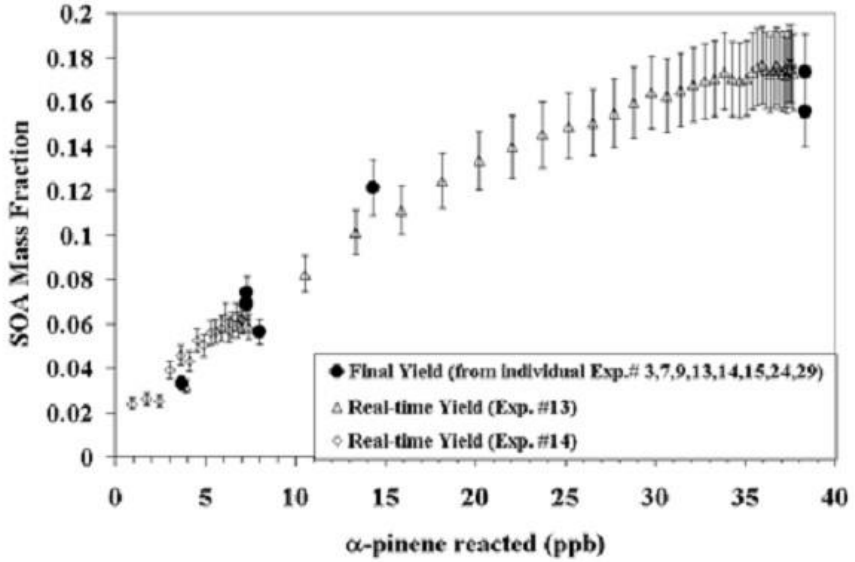

Figure 2.6 SOA Mass Fractions compared to the amount of α-pinene [13]

Hao et al.[13] quantified the mass yields of SOA from α-pinene oxidation with OH and O_3 from a few plant species that emit α-pinene [13]. α-Pinene oxidation by OH and O_3 result in differences in SOA mass yield. Similar to the previous models, OH oxidation proceeds by H-abstraction or addition to a carbon double-bond site. However, O_3 oxidation of VOCs creates ozonide first and then decomposes to form the products. The volatility growth factor (the ratio of the diameter of the particle after evaporation divided by the original diameter) of OH systems is 20-50% lower than O_3 system[13]. Hao et al.[13] found that SOA mass yields for oxidation α-pinene from biogenic sources were around 10 ± 2%. This was similar to the result Pathak et al.[12] found for α-pinene oxidation.

2.3 Instrumentation

In order to study SOA and emission profiles, an instrument suite was designed and assembled that allows in-situ VOC generation, SOA production, and rapid sampling and analysis. This suite consists of a combustion chamber to produce particles and gaseous species from real sources, a PAM chamber to oxidize the emissions, and a TAG GC/MS to

collect and analyze the emissions. The PAM chamber lamp voltages are variable, changing the extent of oxidation of input material. This allows comparisons of various oxidation states, from non-oxidized to an equivalent exposure of 2-weeks of atmospheric aging. These species are impacted onto the TAG collector where they can be desorbed and measured using a GC/MS. Highly volatile species will not condense/ be analyzed by the TAG system because the collection cell is maintained at room temperature during sampling. Artificial cooling of the cell could allow for collection of more volatile species.

The combustion chamber is critical to these studies, allowing controlled production of source material. The PAM chamber ages samples from the combustion chamber. The combination of these two systems will create particles of a known source and oxidative age. These particles can then be sampled using various methods such as an aerosol mass spectrometer (AMS)[25][26] or thermal desorption aerosol gas chromatograph (TAG)[19] to determine the chemical composition of these primary and secondary sources, or a scanning mobility particle sizer (SMPS)[27] for resulting particle size distributions. Eventually, the goal is to create a chemical profile database of POA sources and various types of SOA and the pathways by which they are created. These individual profiles can then be used for identification purposes when sampling the real atmosphere with a complex mixture of contributing sources. Chemical speciation of more POA and SOA sources will allow for better determination of ambient particle sources and improved atmospheric modeling.

This data can be obtained through laboratory experimentation. Smog chamber and other oxidation experiments measure the amount and composition of the products of these reactions. The conditions under which the experiments take place can shift the balance of the resulting products, such as NOx vs NOx-free systems. Additionally, an OH-dominated system results in higher volatility species compared to an O_3 system [13].

Previous studies have been limited in multiple ways. Smog chambers involve a large container with some method of exposing the contents of this container to UV radiation. Smog chambers normally accomplish this using a clear Teflon bag, ranging in size from lab bench scale up to 250 m^3 or larger[14]. Particles or source gasses are loaded into the chamber before exposure. The chamber is exposed to UV radiation by external UV lights oxidizing the material all at one time. The voltage applied to the lights determines the UV intensity,

which in turn determines the amount of OH radical produced. The sample is aged in this chamber for an amount of time before being sampled using various equipment, such as an AMS. The sampling rate and chamber volume determine how long a single experiment can be conducted. Chamber wall interactions begin to influence the chemical mechanisms after a smog chamber experiment has operated for too long[14].

Since the sample is not all collected immediately, the residence times of the particles change as the sampling elapses. This results in a dynamic measurement. While this offers insight into the aging process, it also requires a long setup time for each experiment and samples at a specific residence time and oxidation age can only be taken once per experimental cycle. Smog chambers are intrinsically a batch system. This is a limitation, because once charged, a smog chamber is only removing sample instead of continuously creating more. Once all of the particles are removed, the chamber has to be charged again. This limits the amount of time over which a sample can be taken. The goal of the PAM and combustion chamber is to address these issues and allow for new methods for oxidation experiments.

A combustion chamber with subsequent oxidation offers solutions to some of the limitations of a smog chamber. By allowing continuous production of particles and source gases, the chamber allows for steady state continuous measurements. The objective of the combustion chamber attached to a PAM chamber is to characterize various emission profiles, both oxidized (SOA) and primary emissions, from a controlled source and over a controlled range of oxidation states.

Currently, the factors generated by positive matrix factorization (PMF), a commonly applied statistical technique to find covariance amongst chemical signatures from various sources [32], are not rigorously compared to laboratory generated single source chemical signatures, especially for aged sources that contain significant secondary species. Ambient aerosol PMF factors can then be tested against source profiles created using controlled production of materials from our laboratory system. Such analysis is critical for verification of source apportionment efforts. The addition of the PAM chamber to this work is critical for determining secondary aerosol chemical profiles.

Potential aerosol mass represents the maximum aerosol mass that a precursor can achieve through oxidation. In the PAM chamber, organic precursor gases are oxidized rapidly to form SOA. The objective is to simulate the photo-oxidation that occurs in the atmosphere. To simulate equivalent atmospheric oxidation (oxidant exposure) and particle formation, all of the processes that occur in the atmosphere over longer time periods must occur over the shorter residence time of the PAM chamber (i.e., a couple minutes, flow dependent). This includes a variety of processes such as the oxidation of precursor gas, nucleation of particles (in the case of a particle-seed free experiment), and re-partitioning of phases [16]. The geometry of the PAM chamber allows for plug flow which offers more uniform aging compared to a smog chamber. The resulting concentrations of OH and O_3 are positively correlated with the UV exposure of the system (controlled by lamp voltage), and there is a direct correlation between the formation of SOA and the presence of OH and O_3 in the PAM chamber [16]. Kang et al initially demonstrated the relationship between oxidant exposure and SOA generation in the PAM chamber (see Fig. 2.6) [16]. In addition, notice how the humidity also affects the production of SOA. In the cases of higher humidity, there is also a larger amount of SOA.

The layout for a PAM reactor is straight forward. A cylindrical flow tube made from treated aluminum was fitted with adjustable UV lamps. These lamps were placed in Teflon sleeves and produce the ozone for the oxidation process. Sample can be continuously passed through this reaction chamber. If the flow through the tube is held constant, a mean residence time can be determined. This allows the average age of the particles to be calibrated to the input voltage (intensity) of the UV lamps, where relationships between voltage and resulting O_3 and OH concentrations are determined over a wide range of voltages and oxidant production. O_3 is directly measured and OH is inferred using reaction kinetics applied to the depletion of an input SO_2 calibration gas. The residence time distribution is important because a more narrow distribution results in a more uniform particle oxidation state.

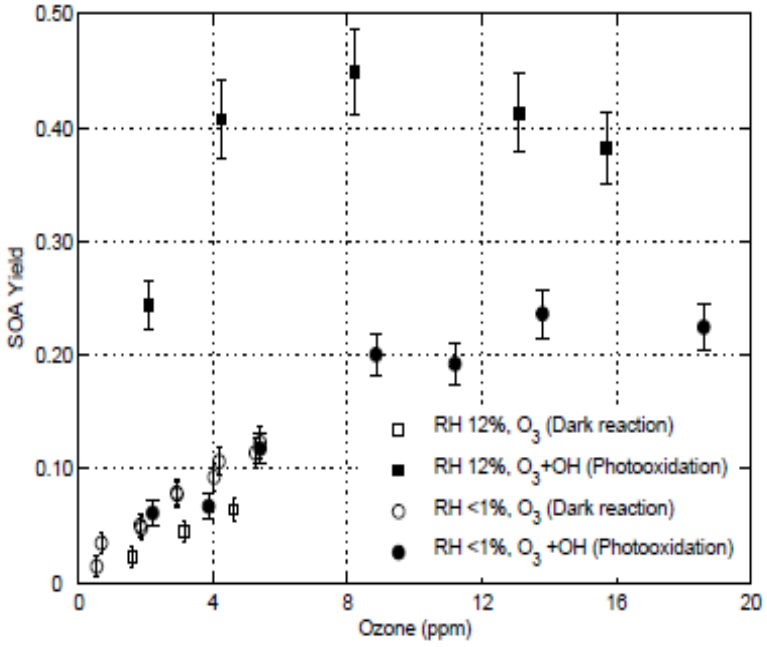

Figure 2.7 SOA yield compared to Ozone concentrations[16]

A study by Lambe et al.[14] compared 2 different models of oxidation flow tube reactors. These were the Toronto Photo-Oxidation Tube (TPOT) and the PAM flow tube reactors. The two were also compared with a smog chamber in order to compare the effectiveness of these methods. TPOT and PAM differ in purpose. The TPOT was originally designed for high OH concentrations to be used in heterogeneous oxidation experiments (particle aging), while the PAM system was designed to study the formation of particles from gas[14]. In this experiment, the PAM system was a larger system, allowing for longer residence times for the same flow.

The systems were compared on a number of criteria including particle and gas transmission efficiencies, and the residence time distributions. PAM had lower losses in the gas phase. The particle transmissions were similar in TPOT and PAM. The TPOT had a narrower residence time distribution than the PAM. This would result in the TPOT having more consistent outflow than the PAM. This is likely due to the length to diameter ratio; TPOT has a larger ratio than PAM[17]. The result of this paper was that the choice between the two systems came down to application. In the case of aging of organic gasses and particle formation, PAM works very effectively. Therefore, a PAM chamber was chosen to be used in conjunction with the combustion chamber in our research laboratory.

The original PAM design utilized a suspended Teflon bag. UV grid lamps acted as the light source. The system was redesigned as a solid chamber tube to address several issues with the prototype design. Two forms are primarily used currently, a metal cylinder and a Pyrex cylinder. In the original design there was a wide range of residence times. The new design delivers better residence time control. In addition, the new chambers are more portable and more durable. This is crucial if the systems are going to be used in field studies. Other labs using the PAM chamber include Prof. Willam Brune's group at Penn State University, Prof. Jose Jimenez's group at University of Colorado-Boulder, and Prof. Paul Davidovits' lab at Boston College. None of these groups have integrated the PAM with a TAG system and Combustion Chamber as we have. This affords us some unique experimentation opportunities.

My research primarily focused on the construction and preliminary characterization of a combustion chamber for laboratory studies, purchasing and setup of various laboratory equipment (e.g., monitors for O_3, SO_2, $NO/NO_2/NOx$), and development of control systems for both the TAG sampling system and the dual PAM/combustion chamber system. In addition, preliminary studies were conducted to start creating a portfolio of oxidation profiles. This chamber will be a critical piece of equipment in characterization of secondary organic aerosols (SOA) and source profiles.

Chapter 3

Development

Development of the PAM, TAG, and Combustion Chamber can be divided into two stages. The first stage (Instrumentation) included construction of the physical systems, and the second stage (Controls) included development of the control systems. The second stage includes development of both the control hardware and control software.

3.1 Instrumentation

3.1.1 Combustion Chamber

The main constraints on the combustion chamber are as follows. The chamber has to be able to operate at high temperatures without damage. It also must be non-reactive at these temperatures. The chamber must also be large enough to allow sampling at the rates required for a TAG system in combination with other sampling instruments (e.g., 15-20 liters per minute). Finally, the chamber must be easy to operate and maintain, and must meet basic safety requirements. This means that samples are easy to set up and remove. This also means that during the experiments, the chamber is able to be visually monitored to prevent flare-ups for example.

Due to the intended purpose of combusting material inside the chamber and measuring emissions, it is critical for the chamber to be constructed out of materials that would not release any gases or particles when heated. The final combustion chamber has tempered glass walls, an aluminum floor and ceiling, and aluminum frame (80/20 Inc., Columbia City, IN). The combustion chamber is divided into two separate compartments by an aluminum panel with a connection hole to allow transport. The tempered (increased safety and strength) glass was chosen because it would allow monitoring of the contents of the chamber. The glass had to be heat resistant as well as notched at the corners in order to allow fitting with the framing. Custom glass panels were ordered from Gravois Glass (St. Louis, MO). A diagram of the combustion chamber is provided in Fig. 3.1.

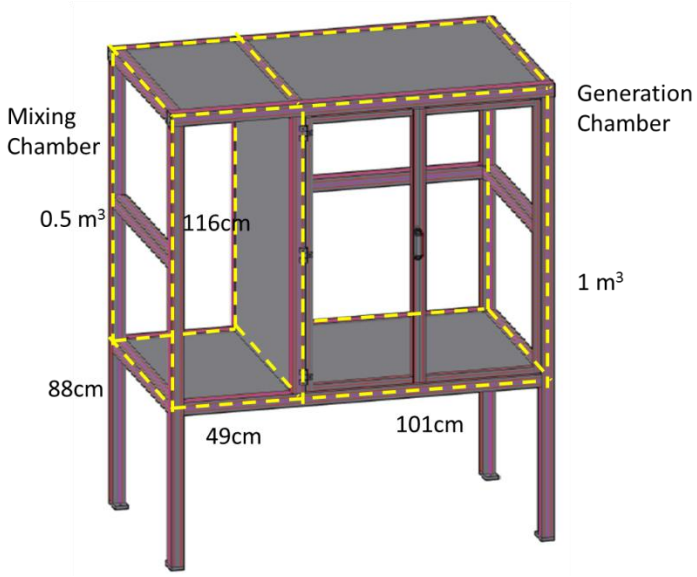

Figure 3.1 Design for the Combustion Chamber

There were a few design issues that had to be fixed in the combustion chamber post construction. The assembly of the side mixing chamber would result in a closed off chamber that could not be cleaned. In addition, it would have been impossible to complete this chamber due to the bolts being placed on the inner walls. Therefore, a door was designed for the side chamber. Initial design called for 2 panels stacked on top of each other. By offsetting these panels, the glass sections could slide past each other, allowing entry. This meant reordering 80/20 framing for a portion of the side wall. A vent was also added to the top of the chamber for continuous ventilation and periodic chamber flushing. A bi-folding door was designed for easy access to the combustion chamber. After construction and testing, it was found that the bi-folding door did not seal well. It was replaced by 2 independent swinging doors. With this adjustment to the door and additional Teflon tape between glass panels and the 80/20 frame slots throughout the chamber, the entire chamber is well sealed.

Upon completion of the expansion of the slots, construction commenced. The general plan was to first construct the bottom portion and uprights, slide the glass panels into the frame, insert the metal dividing wall (with holes drilled to connect the two chambers), construct the chamber door, then install the top section which had been constructed separately. Inlet and outlet holes with Swagelok fittings were installed on both

the top and the bottom metal panels. A filter and ball valve were installed on the purge stream before leading to the outlet vent from the room. Currently, house air that has been further purified using an activated carbon trap and HEPA filter is introduced to the combustion chamber to provide clean background air.

The combustion chamber was constructed inside of a separate room inside the main laboratory. The chamber dimensions are larger than the door to the room, so the chamber would have to be dismantled and reassembled if it is ever needed to be removed. This room was designed with negative pressure to ensure that any gases or particles that may escape the combustion chamber during operation are not allowed to transfer to the main laboratory. A final image of the chamber after assembly is shown in Fig 3.2.

Figure 3.2 Combustion Chamber After Assembly

The key dimensions of the chamber are as follows. The combustion chamber measures 101cm wide by 116 cm tall by 88 cm deep. This results in a volume of approximately 1 m^3. The mixing chamber has the same depth and height but was only 49 cm wide. This resulted in a volume of approximately 0.5 m^3. The total volume for the system then is approximately 1.5 m^3. Sample from the combustion chamber is delivered to the PAM chamber.

3.1.2 PAM Chamber

The PAM chamber was constructed by Prof. William Brune's group at Penn State. The PAM chamber consist of a treated aluminum cylinder 18" long and 8" in diameter. There are 2 ports for 12" BHK mercury lamps. These lamps are surrounded by clear Teflon sheaths. The mercury lamps emit light with wavelengths of 185nm and 254nm. These wavelengths enable: 1) O_3 production from O_2 photolysis by 185nm light, and 2) production of OH from adding external excess O_3 and H_2O, where O_3 then photolyzes from both wavelengths to produce excited $O(^1D)$ which attacks H_2O to form 2 OH molecules. Excess external O_3 is generated by passing pure oxygen past a 2" lamp prior to the PAM chamber. In order to prevent further O_3 production inside the PAM chamber, the Teflon sheaths in the PAM chamber can be replaced by quartz sheaths. This filters out the 185nm wavelength allowing only OH production from method 2 above. The sheaths are filled with N_2, surrounding the lamps, in order to prevent any material contamination on the lamps. The N_2 flow N_2 is also added to the PAM chamber as an inert carrier gas. This N_2 is first humidified in order to provide the necessary H_2O for the OH production. Input N_2, O_3, H_2O, and sample (either from the combustion chamber or of pure test gases such as α-pinene) are delivered to the PAM chamber for controlled oxidation. The rate of oxidation in the PAM chamber is dramatically faster than the natural aging that takes place in the atmosphere.

The reaction generating O_3 and OH are shown. The light produced by the mercury lamps (wavelengths 185nm and 254nm) allows these reactions to take place as indicated by the presence of photon energy in the reaction equations.

$$O_2 + h\nu \rightarrow O + O \qquad h\nu < 240 \text{ nm}$$

$$O + O_2 + M \rightarrow O_3 + M$$

$$O_3 + h\nu \rightarrow O_2 + O(^1D) \qquad h\nu < 320 \text{ nm}$$

$$O(^1D) + M \rightarrow O + M$$

$$O(^1D) + H_2O \rightarrow 2OH$$

Following the PAM chamber it is necessary to remove O_3 to prevent it from corroding the internal components of the measurement devices. An O_3 denuder was built in order to remove O_3 without particle loss. The O_3 denuder consists of a 2 ft long polycarbonate tube filled with Carulite ® 200 (Carus Corporation), an O_3 scrubbing material. In the center of the denuder is a perforated tube to allow gases with a high diffusion rate (e.g., O_3) to travel outward and absorb onto the Carulite ® 200. Particles, with slower diffusion, will pass through the center of the denuder. End caps were machined in the Chemistry machine shop at Washington University in St. Louis. Sample semi-volatile gases and nonvolatile particles are then delivered downstream to be collected and analyzed by physical (e.g., SMPS/CPC) and chemical (e.g., AMS, TAG) measurement systems.

I actively participated in initial plumbing of the PAM chamber, installation of UV lamps, and construction of the external O_3 generator, humidifier, flow control, and design of the PAM control system (described in the following section on Controls).

3.1.3 TAG GC/MS

The TAG system employs an inertial impaction collection cell to collect fine particles at a flow rate of 10 lpm. Ambient aerosol collection typically takes 30 min, however, laboratory generated aerosol collection for 10 min usually results in ample sample mass. The TAG system offers a major advantage of traditional filter sampling, where ambient sampling typically would require 24 hours of sample collection, and the fully automated TAG system requires no sample handling. Following collection, sample is desorbed in a Helium environment to 300°C and delivered in the gas phase to the head of a gas chromatograph for chemical separation followed by a mass spectrometer for compound identification. Once desorbed, the GC/MS will analyze the prior sample while the next sample is being collected. The TAG was built in the lab following designs from Prof. Brent Williams [19]. The TAG system is pictured below.

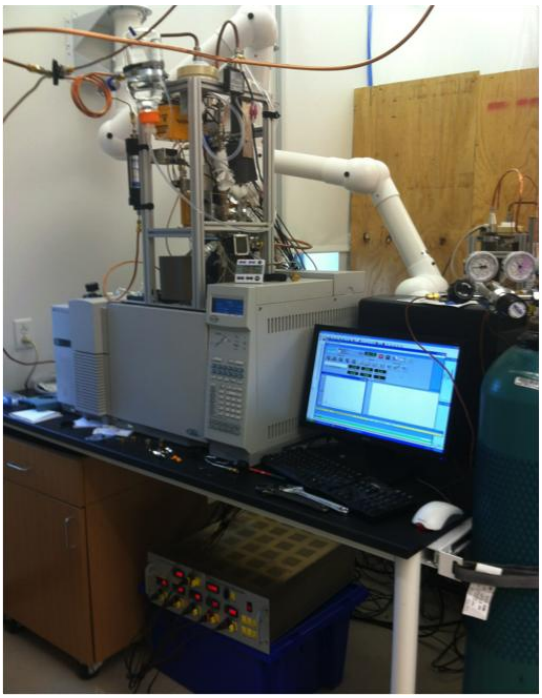

Figure 3.3 TAG System

GC/MS results consist of two parts. The first is the chromatogram. This displays the abundance in sample (ion) response with respect to time. The column in the GC is a non-polar column. Since the column in the GC separates the material based upon volatility, as the time increases, the volatility of the species being measured with the MS decreases. The chromatogram, therefore, shows the abundance at various volatilities. The chromatogram is comprised of multiple peaks signifying various compounds eluting from the column.

The second portion of the results is the mass spectrum. When compounds elute into the quadrupole mass spectrometer, the mass spec applies electron impact ionization and utilizes charged rods to filter ions based upon their mass-to-charge ratio, m/z. This voltage is varied (scanned) allowing various m/z ratios to be detected. From each quadrupole scan, a mass spectrum is created. Each organic species has a unique signature mass spectrum. Species can be identified based upon the mass spectrum that is created. A database of chemical species is used for identification of the species. We use both the NIST 2005 MS database and the Palisade 600K MS database to identify mass spectral signatures.

I actively participated in construction of the TAG collection tower and connection to a commercial GC/MS system (Agilent Technologies, 6890 GC, 5973 MS). I finished the

internal wiring of the TAG control system and performed all communication design, coding, and testing (this will be discussed in more detail in the following section on Controls).

3.1.4 Other Equipment

In addition to the construction of the TAG, PAM, and Combustion chamber, a suite of gas monitors (Thermo Environmental Instruments 42iTL, 43iTLE, and 49i measuring $NO/NO_2/NOx$, SO_2, and O_3 respectively) were required to measure key trace gas species. Ozone levels are critical to know along with OH concentrations. Without these measurements, it isn't possible to know the level of oxidation taking place in the PAM chamber. Ozone can be measured directly. The monitor purchased from Thermo is an ultraviolet photometric analyzer; a mercury lamp passing through the sample onto a photodiode. The amount of absorption of the light allows determination of O_3 concentrations.

Compared to O_3, OH is much more difficult to measure, with very short lifetimes. Due to the extreme oxidation capabilities of the OH, it is necessary to measure its effect instead of the direct concentrations. A scavenger of known concentration (and exclusive to OH oxidation) can be utilized to determine concentrations of the OH by difference of inlet and outlet concentrations. SO_2 reacts with OH to form sulfuric acid with a known reaction rate ($k = 1.2*10^{-12} cm^3 molecule^{-1} s^{-1}$). Therefore, a SO_2 monitor is employed along with an O_3 monitor. The SO_2 monitor uses pulsed UV fluorescence. SO_2 absorbs UV light, exciting the SO_2, then reemits the energy at a different wavelength. Measuring the new wavelength allows concentration measurements. With a direct O_3 measurement and indirect OH measurement, it is possible to approximate an equivalent aging time in the system.

As shown in the α-pinene studies, NOx concentrations greatly affect the SOA yields. A NOx (combining NO + NO_2) monitor is also utilized in our gas measurement suite because of this effect. The NOx monitor allows speciated measurements of NO and NO_2 concentrations. Only one of the compounds is directly measured (NO). The other (NO_2) is first converted, using a molybdenum catalyst, to NO. This allows the concentration of NO_2 to be determined by taking the difference between the NO measurement and NO+NO_2 measurement, acquired by cycling the sample stream in/out of the catalyst. The final measurement is made using chemiluminesence. This occurs by the reaction of NO with O_3

forming an excited product. This product, NO_2*, will emit energy, *hv*, and return to a stable form. Measuring the released light energy allows concentration measurements.

I worked with Thermo Scientific to design a combined system to suit our needs. The final design included a monitor for O_3 (49i), and trace level monitors for $NO/NO_2/NOx$ (42iTL), and SO_2 (43iTLE). Trace level monitors will allow these systems to be used for ambient field studies as well as laboratory studies. All systems were placed in a single rack with a calibration system (46i), pump, electronics, exhaust manifold, and Ethernet communications junction box (for use of iPort communication). A diagram of the entire system is shown below in figure 3.4 in order to illustrate the connections between the equipment.

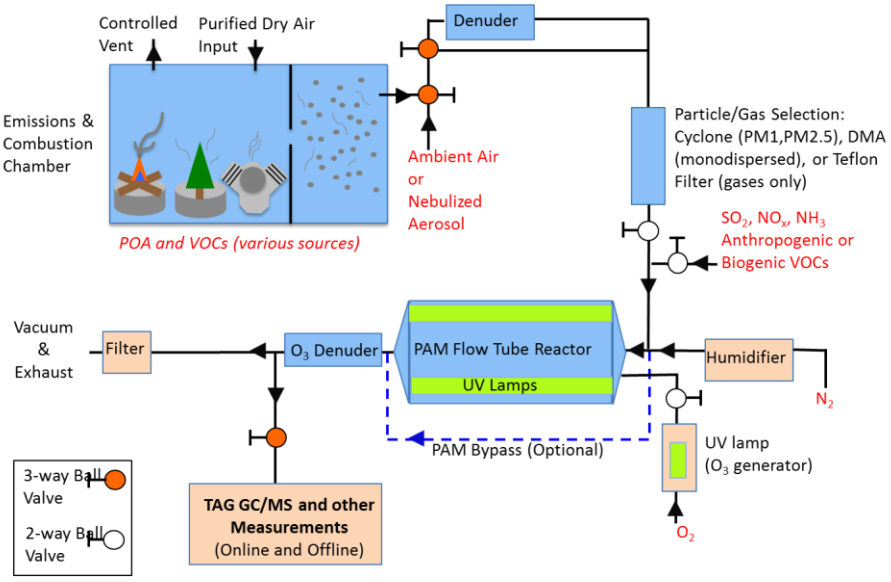

Figure 3.4 TAG/PAM/Combustion Chamber Diagram

3.2 Controls

Control design is divided into 2 major sections, the TAG system and the Combustion/PAM chambers. Each section contains hardware and software components.

3.2.1 TAG Hardware Controls

The TAG control system is pictured below (Fig. 3.5). This system incorporates multiple components. Valves, heaters, flow controllers, PIDs, and various other components are controlled through a single system. Two Ontrak relay boards are used to position the various valves by controlling the power supplied to the valves. Needle valves require one relay. When energized, the valve opens. Ball valves require two relays in order to control them. When one is energized, it holds one position, and when the other is energized it switches to the other position. Each board has eight relays, requiring two boards in order to control all of the valves required by the TAG system. In order to control and monitor external flow controllers, and to record additional thermocouple readings, humidities, and pressures, a National Instruments Breakout PCI-Control board was used.

The NI PCI-6221 control board was selected for the TAG control system. The board has two analog outputs, twenty four digital in/outs, and sixteen analog inputs. The analog outputs control the flow controller. This regulates the helium flow in the system. The analog inputs are used for the various meters, including a pressure transducer, and RH&T sensors. Digital outputs are used to start the GC/MS.

There are seven external PIDs that control temperatures across the TAG system. PID controller stands for Proportional, Integral, and Differential controller. PIDs employ a feedback control mechanism. Feedback control means that the controller determines the proper response based upon a measurement. Using a set-point and a measurement, the PID algorithm determines the load required to achieve the set-point based upon the error. With temperatures, a thermocouple measures the temperature and the error represents the difference between the set-point and the measured temperature.

The TAG has 7 Fuji PXR Temperature Controllers (PXR3-TCY1-4VMA1). Each PID controller has the capacity for multiple set points, hold times, and ramp times. This allows the PIDs to create a temperature profile with time. Using these temperature profiles, the TAG collects material on to the cell at a low temperature then desorbs by heating to 300°C. All PIDs use K-type thermocouples for reading the temperatures. There are several different temperature zones on the TAG system [19] that are all managed using PID controllers with heater/thermocouple feedback.

We are employing multiple heater designs on the TAG system, but all of them are resistive heaters. The Fuji PIDs use digital outputs. This means that they send either a signal for "ON" or a signal for "OFF". This is unlike most PID theory which uses a percent load by way of an analog signal. The Fuji PIDs use digital outputs in a way that creates a similarly duty load. This is accomplished by being on for a portion of the time and off for the other portion. For instance, if the calculated duty was 70% of the heaters capacity, an analog output would send a 70% signal. The digital output is on for 70% then off for the remaining 30%.

In order to take the 5V output from the Fuji PIDs and send a voltage that can power the heaters, a Solid State Relay (SSR) is used. An SSR is a switch that provides a way to take the 5V control signal and provide the standard 120V. Unlike mechanical switches, a solid state relay has no moving parts. This allows it to switch rapidly without wearing out or breaking. Solid state relays offer another advantage in that they are electrically isolating the high-voltage power from the controls. When the control voltage is supplied, the SSR will activate an internal switch. This switch is an optical switch using diodes.

The control system is shown below.

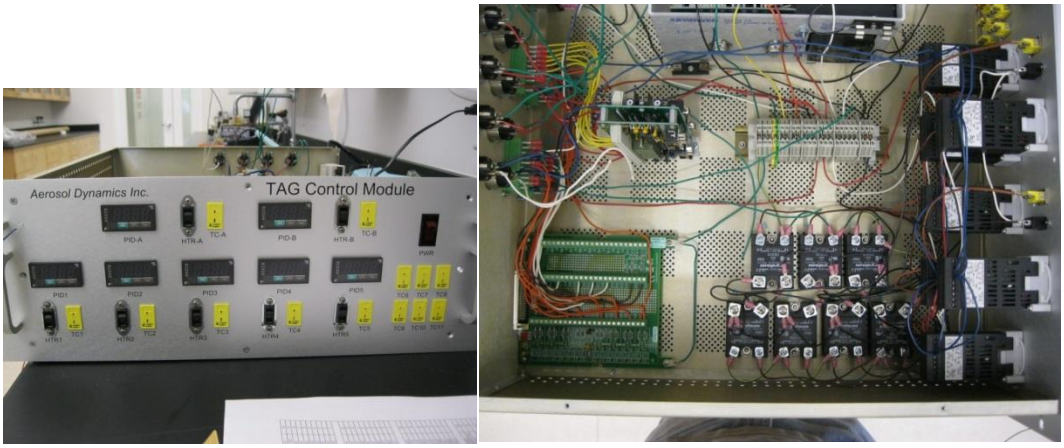

Figure 3.5 TAG Control Box

In order to operate the TAG system, 2 control programs are used at the same time. The Agilent GC/MS is operated with ChemStation. This program controls the temperature cycling for the GC, as well as collects the data from the quadrapole mass spec. ChemStation ramps the oven temperature causing volatility separation in the GC column. We can then

analyze the mass spectra to identify the species in the sample and create profiles for the various emissions. Chemstation is a commercially available control system designed to support the Agilent GC/MS. The second control program is for the operation and recording of the TAG collection/desorption cycling. I actively participated in redesigning and testing this program specific to the WashU TAG system.

3.2.2 TAG Software Controls

The hardware for the TAG Control Module (TCM) is controlled through National Instruments Labview 2011. The original TCM was designed by Aerosol Dynamics Inc. (Berkeley, CA). There have been many updates in the past to allow additional functionality and ease of use. Labview is a graphical programing language that allows useful instrumentation control panel design. Labview programs are comprised of two sections. There is a front panel, where the controls can be operated, and a back panel, where the program for the controls is written. The front panel is shown below.

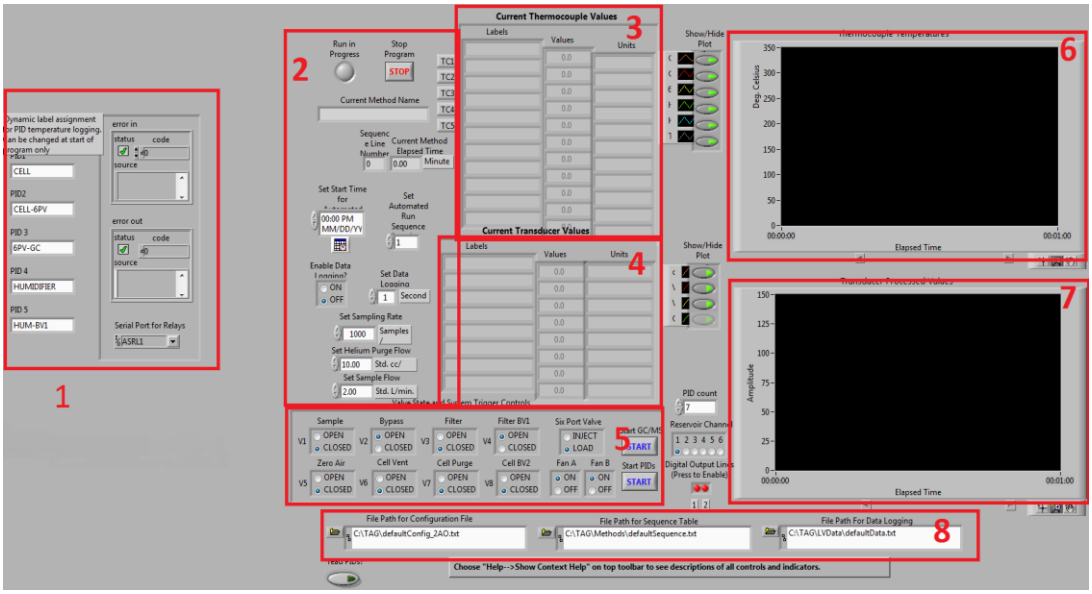

Figure 3.6 TAG Control Software Front Panel

The various sections of the front panel are highlighted above. When the program starts, a dialogue option will offer the choice between automatic and manual. Selecting automatic will start a run as selected in the Sequence. Manual will operate the TAG system but will not make any state changes without manual selection.

Section 1 labels the PIDs, reads the errors, and assigns the serial port for the relay boards. The PID names are then read out to section 3 where the temperatures are listed for each thermocouple/PID. Errors are an important way to understand issues in operation and programing. When an issue occurs, it is displayed here to assist with debugging of the program or operation procedure.

Section 2 controls a lot of the operations. The program can be stopped by pushing the stop button. If a run is in progress, the indicator in the up right corner will be green. The name of the current method will be displayed below. The method run time is also shown. In this section is also the control for setting automatic start time, data logging intervals, and sampling rates. The automatic start time must be at a time after the program is started or else the run will not start and will display an error. Purge Helium and sample flow can also be controlled here.

Section 3 displays the current thermocouple temperatures while section 4 displays pressure, flow rates, humidity and other parameters. These two sections are also plotted over time in the two graphs to the right, section 6 and 7 respectively.

Section 5 has all of the relay positions. It is possible to manually change the valve states here. During an automatic run, the valve states will change automatically. When operating the 6-port valve relay, it is critical that the valve is at 300 C before any movement of the valve, or the valve rotor will be damaged. The GC/MS and PIDs can also be started here, starting the predetermined temperature runs.

Section 8 selects the configuration file, sequence file, and the location for data logging. Configuration files tell the TAG what measurement devices are attached and where to find them. The sequence table is used in automatic runs. The sequence table reads out a list of methods. Each method contains times with various relay states, flow rates, and other controls. When these times are reached in the run, the listed relay values, flow rates, and controls are activated. This is how the automatic runs are controlled. By programing various methods it is possible to create different measurement cycles (e.g., collect and desorb ambient sample, or collect and desorb filtered ambient sample, or run a blank desorption without collection). The data logging address tells the TAG where to write all of the temperatures, pressures, and other engineering information.

The back panel of the Labview TAG control program is shown in appendix A. Labview programing is a visual programming system. Operations are represented by block and data is between blocks via connection lines. The above program is written from left to right. The program is broken down into sections.

On the far left, the program starts by initializing the data structures. This involves loading the configuration files and creating all of the channels for the thermocouples, digital outputs, analog outputs and other input/outputs. These channels define locations of each component. This allows the system to communicate with all components involved. The system builds arrays for the data to be collected. After creating and naming the channels, there is a check to make sure that there is one of each type. If there isn't at least one thermocouple, one analog input, one analog output, and one digital I/O, the system will return an error and stop the program. This is to ensure that later on, the computer does not try to write or read a piece of equipment that does not exist.

Plots are created in the next section. These are the plots in section 6 and 7 on the front panel. Each line being graphed has its own trace which can be turned off or on. The chart parameters can be changed on the back panel. The auto-run start time is also programmed here. The check for the automatic start time is also here. This can be modified so that instead of reading an error if the time has passed, the run starts when the check sees the time has already happened. The master method table and current method are also created here. This creates an array of all the methods and when they will occur.

Now that the channels and plots have been created, the TAG system takes the channels and creates tasks. These tasks are read by the read/write sub VI's. A sub VI is a program (function) inside of the overall program. These are a useful way to create code that can be reused across multiple different programs. These sub VIs can be edited and will open up in Labview when selected. For the analog channels, the information is specified when the channels were created. The tasks include the scaling factors needed to interpret the values for the systems. The first analog output block creates the task for the mass flow controller. The second creates the transducer tasks. The digital I/O's still require more information. This is specified as the task is created. The physical device, ports and lines are specified.

The clock is next. This controls the sampling rate and timeout. The sampling rate sets how often the TAG system will measure and send information. The timeout is a way that the system stops if it gets stuck. If at any point the amount of time set by the timeout happens between sending a signal and receiving one, the timeout error will happen.

Following all of the setup of the earlier stages, the system enters a While-Loop. Loops will continue until a condition is met to conclude the loop. This means that any operation inside of the loop will repeat itself. All previous steps are only run 1 time. Inside the while loop the system is broken down into a few major parts. The most external loop reads in the method sequence and files. The next loop tracks the number of iterations that have been executed. Each iteration of the loop corresponds to one line in the method, or one sub-method. The plots are also conducted in this layer. Data from the internal loops is displayed there. When the master method array has been finished, this loop stops and the program starts to close.

Inside this loop is a stacked sequence containing the major operations of the system. All of the reading and writing takes place here. PIDs are started by sending a start signal inside here. The signal was originally sent in ASCII, however after extensive research it was found that the WashU PID controllers do not read ASCII. The PIDs read and write in Modbus. ASCII and Modbus are communication protocols. In order to describe the differences and implications there in, it is necessary to understand data formats. Four basic forms of communication are Basic, Decimal, Hexidecimal, and ASCII. On the simplest level, communication can take place in Basic, 1s and 0s. Decimal communicates in standard numeric, 0-9, or base 10. Hexidecimal is base 16, with valid characters of 0-9, A,B,C,D,E,F. ASCII is base 256. This means that there are 256 valid characters with each character having a value somewhere in that domain. Modbus uses Hexidecimal communication. An example of a Modbus command and the corresponding Ascii command are shown below. This command would start the ramp/soak cycle of PID 01.

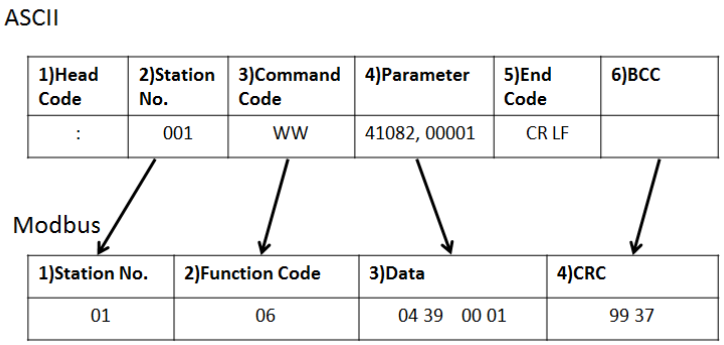

Figure 3.7 ASCII to Modbus Command for Starting a Ramp Cycle

As can be seen, there are 6 sections in ASCII code. The first is the head code. This tells the instrument receiving code that it will be receiving a message. Second is the station number. In the case of the PIDs, it indicates which PID is being talked to. Third is the command code, which tells the instrument whether it is receiving a command or reading out information. Fourth is the parameter value. This is the piece that tells the instrument what to do, such as read temperature or change the PID parameters. Depending upon the register being read/ written, the remaining parameter values have different expected forms. For temperature set point, the number entered will reflect a temperature in degrees Celsius by default. Fifth is the end code, which tells the system that it's the end of the message. Sixth is the Block Character Check. This is an error check to ensure that the data is sent correctly to the instrument. BCC is calculated based upon the rest of the message. Each character in the station number, command code, parameter, and end code are added up to create a single number. The last byte of this summation is the BCC. The instrument will also calculate a BCC value. If they do not agree, this indicates an error in the message transfer[29].

The Modbus protocol is similar. It is comprised of 4 sections. First is the station number, similar to station number in the ASCII protocol. Second is the function code. This is similar to the ASCII command code. It tells the system whether it is reading or writing. Third is the message. This is where the PID is told what register to read or write and what the content of the writing is. Fourth is the CRC, cyclic redundancy check, an error check code. This is similar to the BCC in ASCII, serving the same function, but is slightly differently. A flowchart of the Modbus error check calculations is shown in appendix C. These differences in the protocol result in the ASCII command not being directly

convertible into the Modbus protocol; instead the command has to be rewritten using the correct Modbus formatting[30].

With the inputs being different for the different protocols it was necessary to create new read and write sub VI's for Modbus. The actual command to start the PIDs changed along with the message to tell the PIDs to read out the temperature. When the PIDs receive a message, to write a code or to read out the temperatures, the PIDs respond. This response was also in Modbus, and the message had to be translated back into ASCII so that the Labview program could correctly interpret the values.

Each PID is started with this signal once per method. The message to read the PIDs is sent every measurement cycle. These cycles take place one time every second. These signals are sent over an RS485 connection. There are two possible connections, RS232 and RS485. These connections are for a serial connection. The computer port uses RS232. Originally, in order for the PIDs to communicate with the computer it was thought to require a converter. The PIDs are connected to the relay boards, which were in turn connected to the computer. It was possible to bypass the converter by wiring the PID output to Ontrak the relay board which made the conversion internally. With the PID communication corrected, it was possible to control the PID start times and read the temperatures. Because the PID information is stored on the physical PID units, a secondary program was written to allow quick modification of these values instead of manual data entry. This program allows the PID to be selected, and the individual parameters can be changed as desired.

In addition to PID control, the inner loop controls all of the relays. These relays are controlled via sub VI using the Visa Write controls. This sends the various relay states to the relay boards which attempt to change the state of the relays. If the relays do not switch, it will not respond with a switched state. The system will attempt twice before reporting an error. There is also the capacity to control calibration reservoirs through the Labview program. This is currently not in use, however in the future it will be. These will allow the system to undergo automatic calibrations [33]. The final component that is controlled in this loop is the GC/MS start signal. Once the GC/MS has been prepared using Chemstation, it waits for the signal from Labview to start the cycle. Following all the controls, the system

reads out temperatures and relay states. These are reported in the graphs as well as in the data log. However, before the data is recorded, the values are smoothed using a mean average of the signal over a second to remove noise from the signal.

The final component of the TAG control scheme is the closing of the operation. Once all cycles have been completed, the system will shut down connection to the TAG. Closing channels is important because it prevents errors in future runs. Any errors that have been accrued during the cycles will stop the system and report them here.

3.2.3 Combustion / PAM Chamber Hardware Controls

The Combustion/PAM chamber is a much simpler system to control. Where the TAG system had a large number of valves and subcomponents to control, the PAM/Combustion chamber is not as complex. The chamber control system consists primarily of a single data acquisition board. A National Instruments USB-6343 board was selected for its versatility. This board has 32 analog inputs, 4 analog outputs, and 48 digital I/O ports. This board controls the entire system. A flowchart of the PAM / Combustion Chamber system is shown below. This will help to illustrate the control locations.

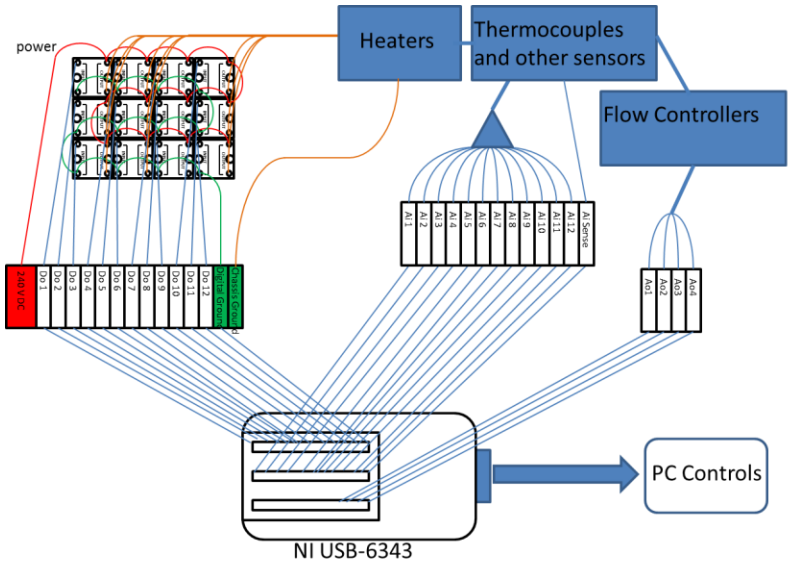

Figure 3.8 PAM Hardware Control System

As can be seen, there are 12 heaters located in the combustion chamber. These are used to volatilize or burn samples to create the emission sources. By combining multiple

different sources at once, various emissions profiles can be created to simulate ambient environments. Single sources can also be heated to various degrees. In order to heat these samples, they are placed in 2.5" diameter stainless steel cups, each with its own band heater. These band heaters could be controlled by physical PID units; however, for this unit it was decided to use software to create the control signals. These signals are sent from the computer through the DAQ board to SSRs, which in turn control the heater power just like the TAG. The software control for this is discussed below. The temperatures are measured using Labview as well. This is accomplished by wiring the thermocouples to analog inputs on the DAQ board. In the TAG system, the Fuji PIDs read the temperatures and reported them to the computer. In the PAM, the DAQ board measures the voltages on the thermocouples and Labview interpret these values in order to determine the temperatures. In addition to the cup and band heaters, there is a humidifier on the nitrogen line before the PAM chamber. The temperature needs to be controlled in order to maintain a specific humidity. This is controlled in the same way as the cups.

Besides digitizing PID controls, the PAM chamber will also control 2 flow controllers and measure relative humidity and temperature (RH&T) at multiple locations. The flow controllers will control the nitrogen and oxygen flows to the system. Nitrogen is used to control the dilution ratios of the sample stream and to ensure quantitative measurements. Oxygen is used for the external excess O_3 generator. RH&T (humidity and temperature) sensors are critical for the conversion of O_3 to OH since H_2O is required. Finally, the voltages of the PAM UV lamps will be controlled through the Combustion/PAM chamber control system.

3.2.4 Combustion / PAM Chamber Software

Labview was employed for the Combustion/PAM Chamber control system. Communication with the DAQ board was the first task. This required editing of some communication protocols since the out-of-box DAQ software did not recognize the board. Using a combination of NI MAX (measurement and automation), Windows Device Manager, integration of various drivers, reinstalling the NI Device Loader and Configuration Manager, Windows 7 was able to recognize the DAQ board. Windows XP required a Hotfix as well. Once communication was established, each type of control was tested. This meant

reading temperatures, RH&T sensors, turning SSRs on and off, and checking various analog outputs.

The front panel for the Chamber control is fairly simple. The temperatures are displayed in the same way as the TAG, with a table of values and a graph of the temperatures to the right. The RH&T, flow rate controls and current flows are listed as well. The PID settings make up the bulk of the rest of the front panel. The P, I, and D parameters for each of the heaters are listed as well as the temperature profiles. Once the system is initialized, similar to the TAG, the various components need to be read. Using tasks, the thermocouples are all read through a single block. This is also true for the RH&T sensors. Flow meters are controlled with an analog output block.

The major difference between the two programs (TAG vs Chamber control) is the use of digital PID calculations for Chamber control. The PID system utilizes subVIs to create the temperature profiles and conduct the PID calculation. The PID calculation follows the same algorithm as the physical units; however, this is all done in Labview instead of external equipment. The subVi that creates the temperature profile takes an array of temperatures and times. It will then output a set point temperature every second to the PID calculation block. What this means is that during the hold portions of a cycle, it will continue to output the same temperature. During the ramp cycles, it will output the correct temperatures to give a smooth ramp cycle, increasing the temperature over the allotted time to the final set-point.

There are multiple different PID algorithms. The standard form of the PID algorithm is as follows:

$$u(t) = K_p * e(t) + K_i * \int_o^t e(\tau)d\tau + K_d * \frac{d}{dt}e(t).$$

In the above equation u(t) represents the duty load output. Kp is the proportional constant, Ki is the integral constant, and Kd is the differential constant. e(t) is the error term. From this we can see how as the error increases, so does the response. The response due to Kp increases linearly as the error increases. The integral error is essentially a collection of the earlier errors. The longer the error has lasted and the larger it is, the larger the integral response will be. The derivative term uses the slope of the error. The more the error is

changing with time the stronger the derivative term affects the output variable. This will result in a more stabilized output, with less overshoot as Kd increases. The table below shows a basic chart of the effects of increasing the tuning parameters.

Table 3.1 Effects of Increasing PID Parameters, [33]

Parameter	Rise Time	Overshoot	Settling Time	Steady State Error
Kp	Decrease	Increase	No trend	Decrease
Ki	Decrease	Increase	Increase	Eliminate
Kd	No trend	Decrease	Decrease	No trend

Using these guidelines it is possible to modify the PID parameters in order to create better temperature responses. The PID block acts as the calculation block. Following the algorithm, it will compute the required heating load. The PID block requires the PID parameters, the set point, the process variable (temperature), and the output range. Output range ranges from 0 to 1, representing 0 to 100% of available power. PID parameters are read from the front panel. The set point is updated from the PID set point profile block.

Unlike the physical PID blocks used in the TAG system, the PID VI blocks output an analog signal. Since SSRs are either completely on or completely off, it is important to convert the analog output into a digital signal. In order for the SSRs to function as a heater, the control voltage needs to be achieved. However, an analog PID can send 50% voltage and still achieve the control voltage. This will result in the SSR being turned on. The method that is best for converting an analog signal into a timed digital output is Pulse-Width Modulation (PWM).

Pulse-Width Modulation is a technique to take an analog signal for a load and convert it into a series of off and on steps resulting in the same amount of load. This is a common technique for electronic inertial devices. The average value of the PWM output will result in the same load as the original analog signal. The duty cycle, or ratio of on time to cycle time, is equivalent to the analog load. PWM uses square pulse waves. The frequency

for PWM must be faster than the response time of the heater. This is to ensure that the system does not spike with the PWM. This cycling should result in the heater turning on and off rapidly causing it to heat slower than it would if it were on continuously. A few examples of PWM are shown below.

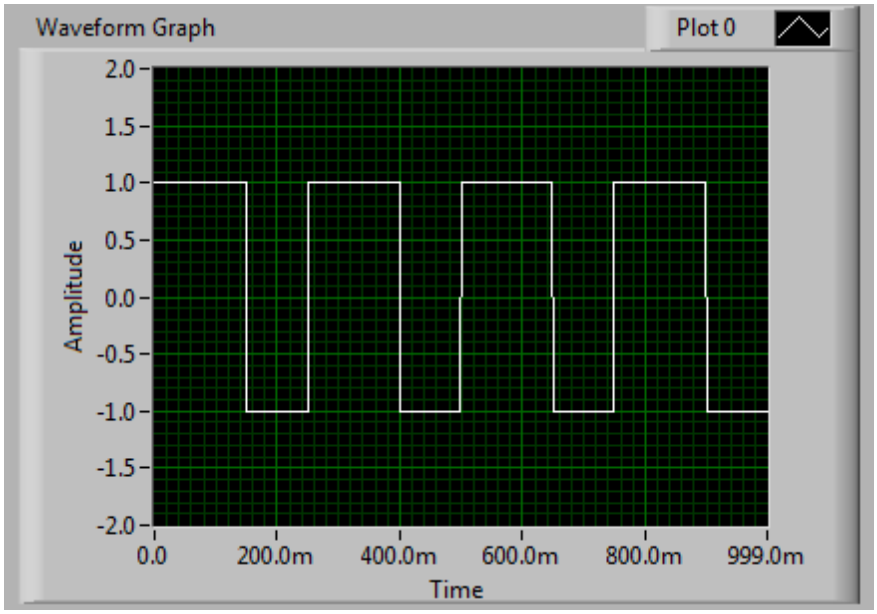

Figure 3.9 PWM Examples

In the above cycle, 4 is the frequency, 1 is the amplitude. The cycle time is 1000min, however this can be set to whatever cycle time is desired. As can be seen, the High Cycles fills a portion of the cycle equivalent to the duty cycle. The high position represents the on position and the low position would represent the off position. It is possible to run PWM with a High, 0, and Low position. For heater control, a negative value does not make physical sense unless a cooling system is added.

Using clock cycles it would be possible to send the on/off cycle to the DAQ board and it would continue to repeat this cycle. However, using digital outputs, it is necessary to send the signal for each cycle. This means that the system cannot simply output the cycle, it must continually send signals. This makes the programming more difficult. It is not possible to run the PWM once per signal; instead the PWM continues to operate making each individual PID requires its own PWM. The PWM block is shown below.

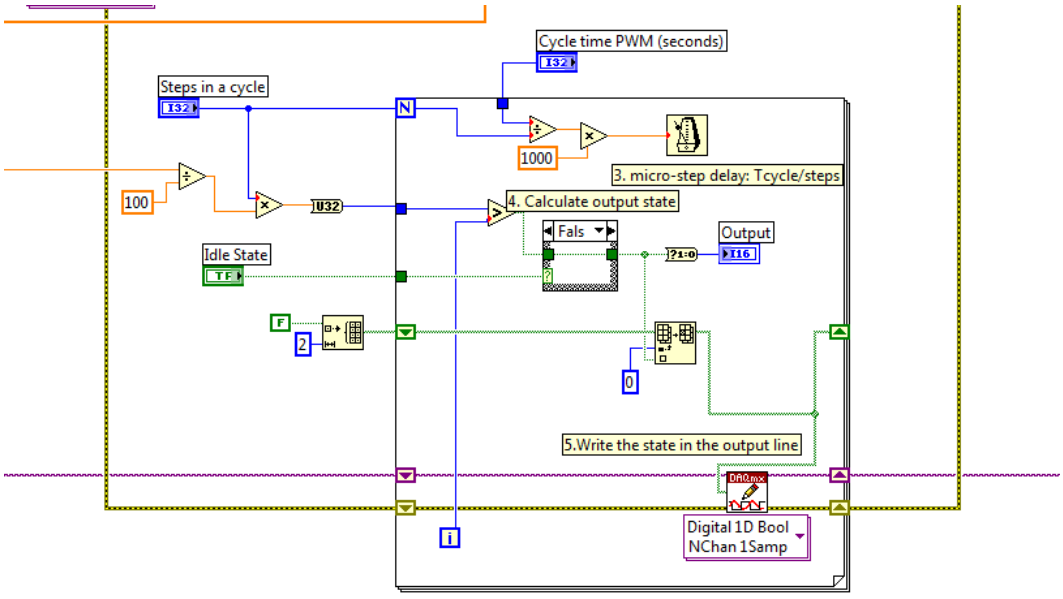

Figure 3.10 PWM Labview Block Diagram

As can be seen, each cycle is made of multiple iterations of a 'For' loop. The start position for each SSR in a cycle is 'On'. Once an equivalent amount of iterations to the duty cycle has passed, the SSR is switched to the off position for the remainder of the cycles. The number of iterations in the 'For Loop' can be changed. An example would be if there were 100 iterations and the duty cycle was 70%, after 70 iterations the SSR would be switched to off. The cycle time of 1 second would result in 1 iteration taking place in $1/100^{th}$ of a second. For 0.7 seconds the SSR would be on, and the SSR would be off for the remaining 0.3. The PWM sends the signal to a digital output on the DAQ board, in turn sending the signal to the SSR controlling the intended heater.

Chapter 4

Experimentation and Preliminary Results

4.1 Combustion Chamber Characterization

Following construction of the Combustion Chamber, initial system calibration took place. The first portion of chamber characterization is determining the residence time distribution for the chamber. In order to determine this, concentrations are monitored leaving the chamber with time. A pulse input of particles into the system generates a single peak. Any deviation from this single peak indicates mixing and reveals insight into the system and its residence time distribution. Background measurements are measured in order to have a reference for when the ground state was achieved after a given experiment. In addition to making preliminary background measurements, a set of procedures for cleaning the systems to achieve the background levels has been provided in appendix E.

In order for the measurements to be relevant to future use of the combustion chamber, the exit flow rate is set to 10 liters per minute. This is the amount that must be removed from the system for a TAG collection. Since the CPC and SMPS being used for these tests only pull 0.3 lpm, a side stream was used to pull the additional 9.7 lpm to the house vacuum system. The side stream was passed through a filter before the vacuum in order to ensure that no particles would be released.

At a flowrate of 10 lpm, with a total combustion chamber volume of 1.5 m^3, the expected residence time is 150 minutes, or 2.5 hours. However, since the combustion chamber is followed by the mixing chamber, the residence time will not reflect the total volume. If the combustion chamber is similar to a Plug Flow Reactor (PFR) and the mixing chamber a Continuously Stirred Tank Reactor (CSTR), we see a delayed CSTR distribution. This would look like a delayed Gaussian distribution. The pulse is generated by combusting a rapid burning material. In the case of this experiment, 3 sheets of large Kim-Wipe tissue were burned. These sheets completely burned within 45 seconds. A CPC and SMPS

measured the concentration over time, at a fixed particle size of 300nm. In the initial sampling, there are not any visible peaks for a long period of time.

The pulses resemble a PFR followed by a CSTR. A sharp peak in concentration occurs with the concentration decreasing rapidly then slowing. This could imply a mixing behavior, deviating from the ideal PFR such as a mixed region prior to the PFR. This could take place inside of the combustion chamber. However, if the original burn emitted a peak of particles right away then slowed down in emissions over time this could explain this shape. The first peak was seen at 1 hour 35 minutes after the initial burn. A PFR of volume 1.5 m^3 would have a residence time of 150 minutes, or 2 hours 30 minutes. The peak is shown below.

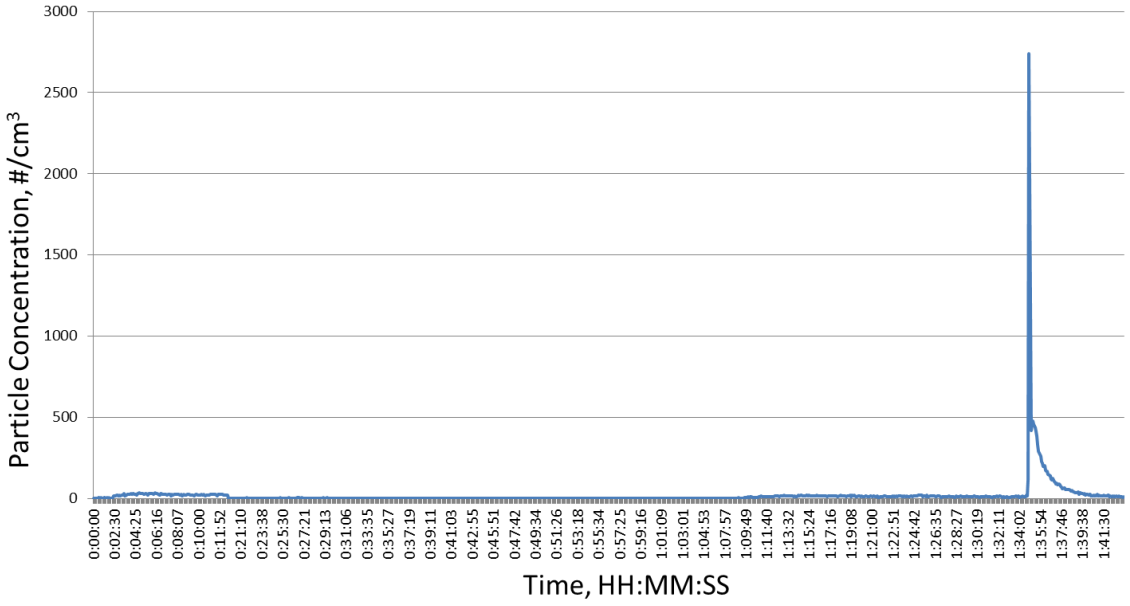

Figure 4.1 Pulse Burn Concentration of 300nm Particles Over Time

If the combustion chamber is assumed to be a PFR and the side chamber to be a CSTR then the residence time was calculated to be 100 minutes at a flow of 10 lpm. This is approximately what was seen here. The shape of the signal in figure 4.1 also agrees with a PFR followed by a CSTR with the deviation from ideal PFR.

An addition set of samples are shown in order to corroborate with the original data. The entire set of data is shown below.

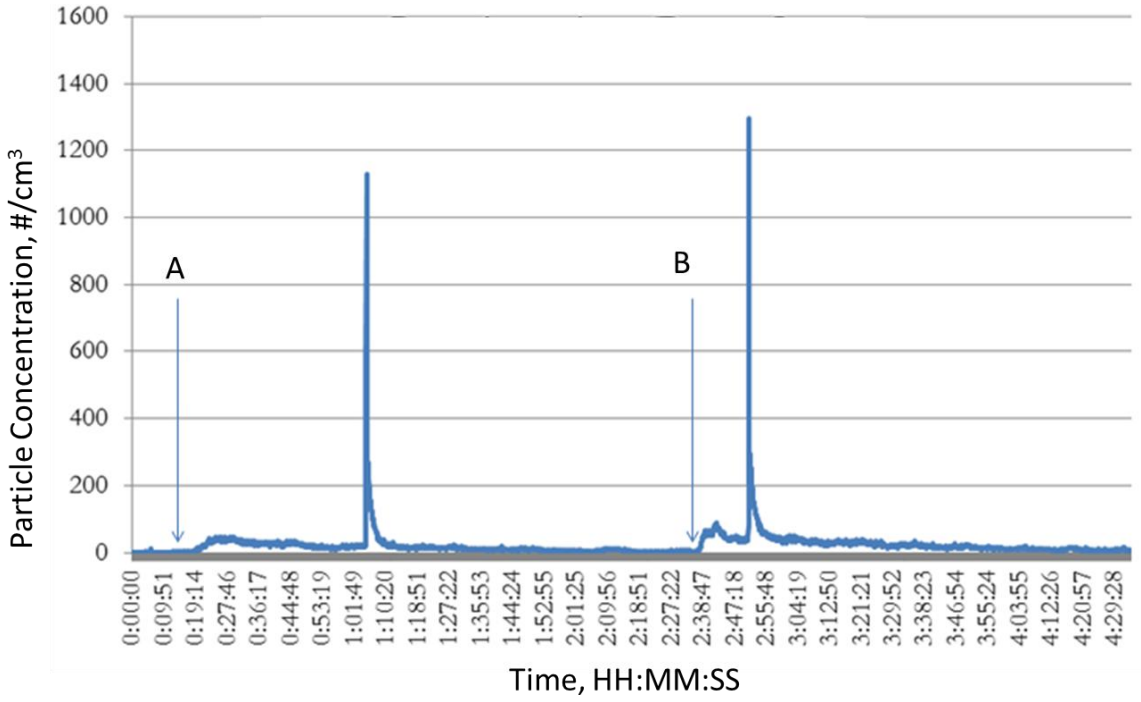

Figure 4.2 Two Pulse Burns In Series, 300nm Particle Concentrations Over Time

In the trial shown in Figure 4.2, the combustions occurred at 0:12, and 2:34 hrs, as indicated by the arrows. The first burn resulted in a peak after 53 minutes. The chamber was allowed to achieve a baseline measurement again before the second burn. However, 15 minutes after the second burn, a peak was seen. The combustion chamber was then allowed to evacuate for a long period of time after this peak. It is likely that sample was travelling out of the chamber and into the mixing chamber by way of leaks in the 80/20 due to the loose fit of the glass panels. The inconsistency in the times of the peaks was of concern.

Combustion chamber (and sub-chamber) flow was tested. Theoretically, this value should be close to 10 lpm because that was the volumetric flow leaving the mixing chamber. However, when a bubble flow meter was attached to the hole between the two chambers, only 0.4 lpm was measured. The mixing volume was clearly not well sealed. Material was being pulled through gaps in the 80/20 framework with sizes approaching that of the hole intended for flow. In order for the chamber to be properly used, a sealant was needed. At the top of the doors, large amounts of particles could be released through the large gap. Teflon non-adhesive tape lined the gaps along the door and in the groves that were open, sealing the chamber. Teflon pipe threading tape was used for small gaps.

Following sealing the chamber, the connection between the combustion and mixing chambers is expanded to increase flow. Vacuum and air lines are added to the chamber, allowing addition air flow through the system. The goal of this is to reduce the overall residence time in the system.

The system was tested for the effects of the evacuation line and the addition of clean air. A fan was also added to the combustion chamber to increases internal mixing. By increasing the chamber mixing, the outputs are both more stable and responsive to changes in the system. Prior to the fan, particle concentrations build up in the top of chamber until the particles are at the level of the sampling port (middle of chamber height). This is due to particles first collecting at the top of the chamber and slowly settling. With the connection to the mixing sub-chamber being halfway down the chamber, this resulted in delayed particle transport. The fan causes these particles to evenly distribute throughout the combustion sub-chamber.

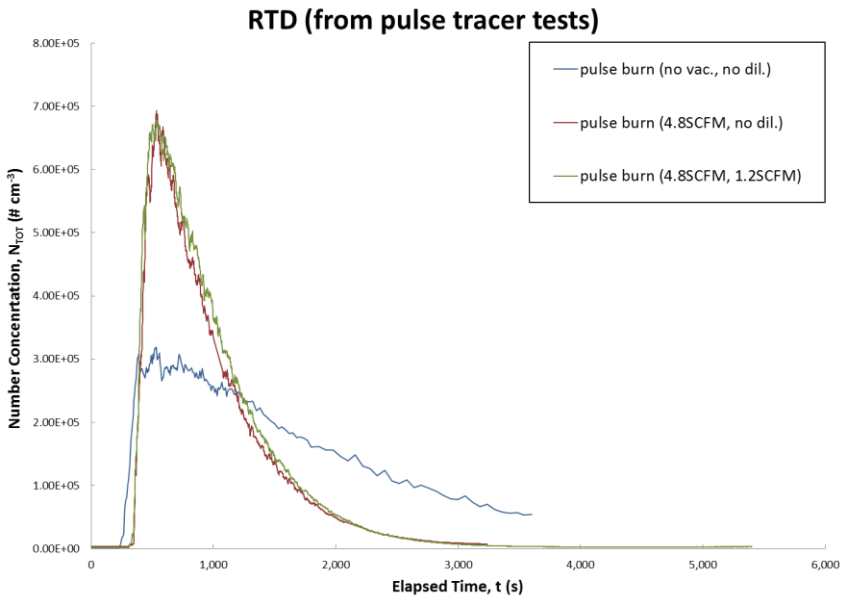

Figure 4.3 Combustion Chamber Pulse Burn Particle Count Over Time Post Modification

Following the chamber modifications, the exit flowrate from the chamber is set to 20 lpm. With the same volume and a new total flowrate of 156 lpm (136lpm from the addition vacuum, 20 from the exit flowrate) leaving the chamber, the calculated residence is approximately 10 minutes. This change in average residence time is reflected in the peak shape observed in Fig 4.3. In addition to cutting the residence time, the time for particles to

reach the detector is greatly reduced by increasing the sampling rate in the chamber and the addition of a fan to quickly mix the combustion chamber. However, as can be seen the addition of the clean air does not greatly affect the measured concentrations. This is because the chamber (which is not completely leak tight) pulls in ambient room air to balance the outlet flow regardless of our additional clean air flow. Particle concentrations in the chamber are much larger than in our laboratory, however, we will always attempt to balance the outlet flow with purified air for future studies.

The purpose of the evacuation line is to allow quick removal of species from of the chamber. With an average lifetime of 10 minutes, over 99% of the material should be removed after 30 minutes. However, as can be seen above this is not the case. After 30 minutes, around 10% of the material seems to still be in the chamber. Increased purified air input would help to clean the chamber more rapidly.

In addition to residence times, the transfer efficiency is tested. This was to ensure that material was not significantly being lost in the connections between the systems. Measurements are taken simultaneously at the exit to the combustion chamber and at the inlet to the TAG system. The particle concentrations did not change significantly between the two locations. This indicates little loss in the sample pipes (3/8" copper) that connect the combustion chamber to the PAM chamber to the TAG system. If there was a high loss, the piping would have to be cleaned and replaced more frequently to avoid buildup. With high transfer efficiency, the piping can be assumed to be fairly clean throughout and only occasionally require cleaning.

4.2 TAG, PAM and Combustion Chamber

Proof of concept for the PAM chamber oxidation is shown by utilizing α-pinene oxidation measured by SMPS. α-Pinene is injected into the nitrogen line upstream of the PAM chamber. 2μL was injected through a high-temperature septa. This α-pinene volatilizes and is carried by the humidified nitrogen. First, a sample was measured without the lamps being on. In the lamp-off position, the α-pinene should remain in the gaseous state and produce no particle mass. With any background particles being present, some of the α-

pinene could condense onto those particles; however most should remain in the vapor phase.

Upon the lamps being powered on, the OH production reaction commences. The oxidation will then begin for α-pinene. This will result in α-pinene producing semi-volatile and non-volatile condensable species. The change can be witnessed in the particle size. As the lamp voltages are turned up, the particle size grows as can be seen below. This illustrates that the α-pinene is in fact oxidizing and that the PAM is functioning. When there was no O_3 or OH oxidation present, the particle counts are very low, indicating the presence of very few background particles. Given the high a-pinene concentration and low pre-existing particle concentration, it is likely that the observed SOA particles during oxidation were formed through nucleation and subsequent growth. This can also be seen below in figure 4.4.

A)

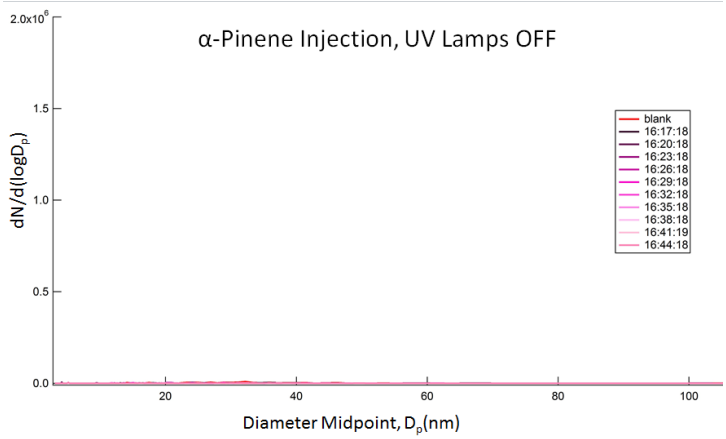

B)

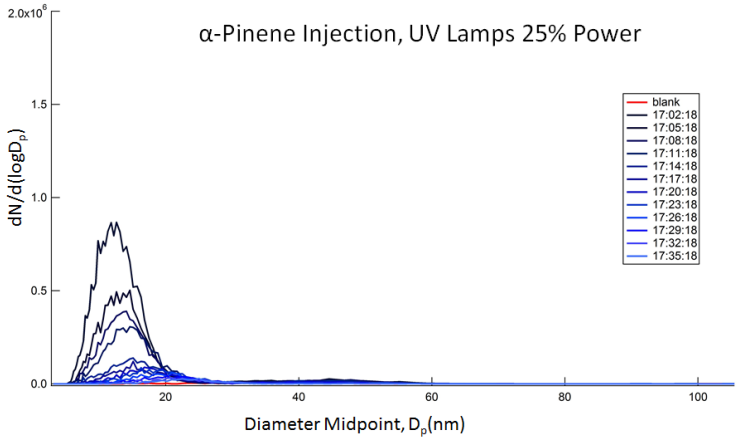

C)

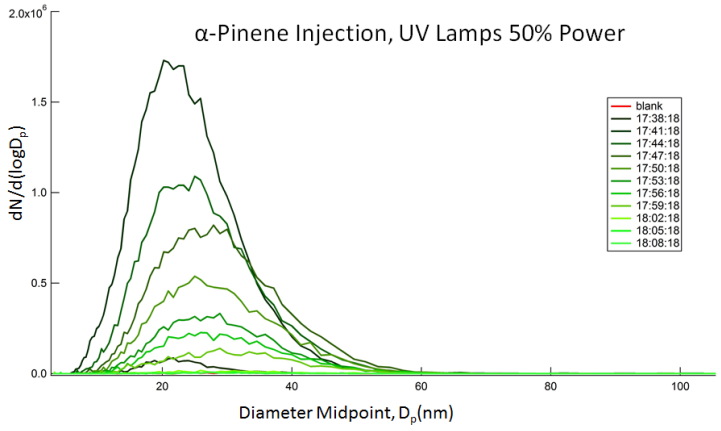

Figure 4.4 SMPS Readings of 2μL α-Pinene Injections at Various Oxidation Levels

In addition to SMPS data, TAG data is also recorded. By running the α-pinene through the TAG, this allows speciation for the α-pinene oxidation products. Due to α-pinene being a volatile species, it does not collect well in the TAG collection cell. Therefor it can be expected that the α-pinene will not show up in the GC/MS data. Once the lamps are turned on, the α-pinene oxidizes, creating secondary species. These can be compared with the expected values from the predictive models and experimental results from other work; however, we did not calibrate the system for our preliminary studies.

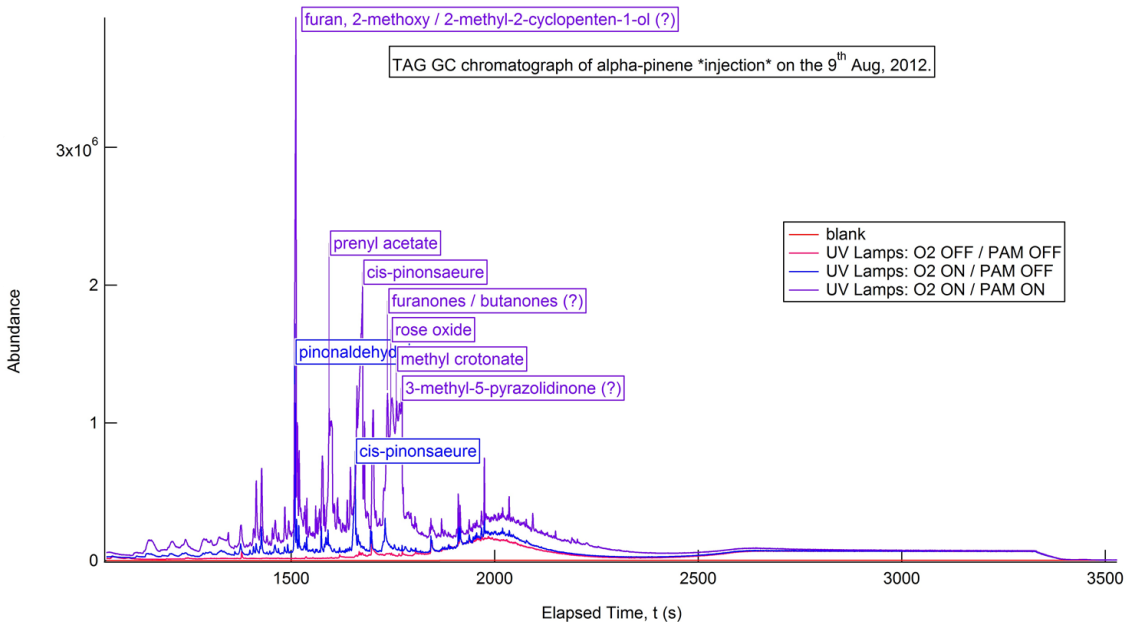

Figure 4.5 α-Pinene Chromatograms

With no oxidation, individual compounds were difficult to isolate due to the low signal. The strongest signal corresponds with the pinonaldehyde, which is a compound found by many of the models, and is commonly applied as a marker compound for a-pinene oxidation in the atmosphere. One area of potential issue with the TAG data is that the TAG is not an effective collector of particles less than 70nm[19]. Looking at the SMPS data, almost all of the particles, by count, are less than 70nm. Particle mass concentrations would include more of the distribution above 70nm, and those are the particles efficiently collected by the TAG system. This brings up the potential issue of the TAG not accurately depicting the chemical composition of the sample. This is an area to be investigated in future experiments, and may require some technique to force the particles to larger sizes. To

illustrate the mass spectral capabilities of the TAG system, the fragment pattern for pinonaldehyde as measured in the above oxidation studies is shown below.

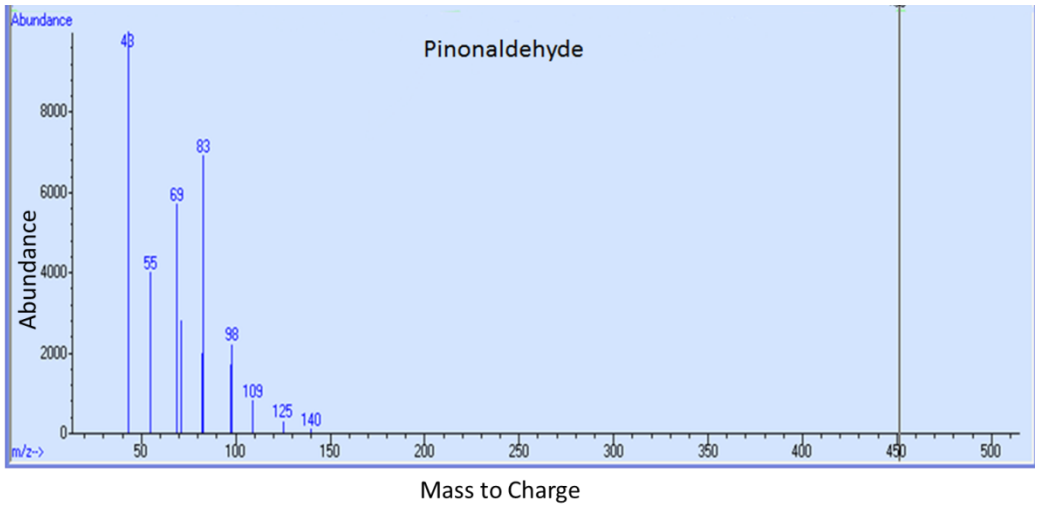

Figure 4.6 Example Pinonaldehyde Mass Spectrum

Preliminary biomass combustion and oxidation was performed using the Combustion Chamber/PAM Chamber/TAG sampling train. Various biomass samples were collected from Tyson Research Center outside of St. Louis, MO. Samples from Oak, Maple, and Pine trees were gathered. Both leaf matter and branches were collected. Tyson Research Center also had some dried wood material as well that had been cut previously. These samples were brought back to the lab and processed in order to allow the combustion chamber to controllably burn the material. This involved grinding of the wood down to sawdust size and crushing leaves. The goal was to make fairly homogenous samples that could reproducibly create similar amounts of smoke over time.

Calibrating the TAG GC/MS will be critical for future studies. An even alkane standard (10ng each of even-numbered C8-C40) is shown below. This illustrates the ranges of sizes of alkanes that can be sample and analyzed by the TAG system. For ambient studies, mixtures of hundreds of known nonpolar and polar species of varying volatilities will be used for TAG calibration.

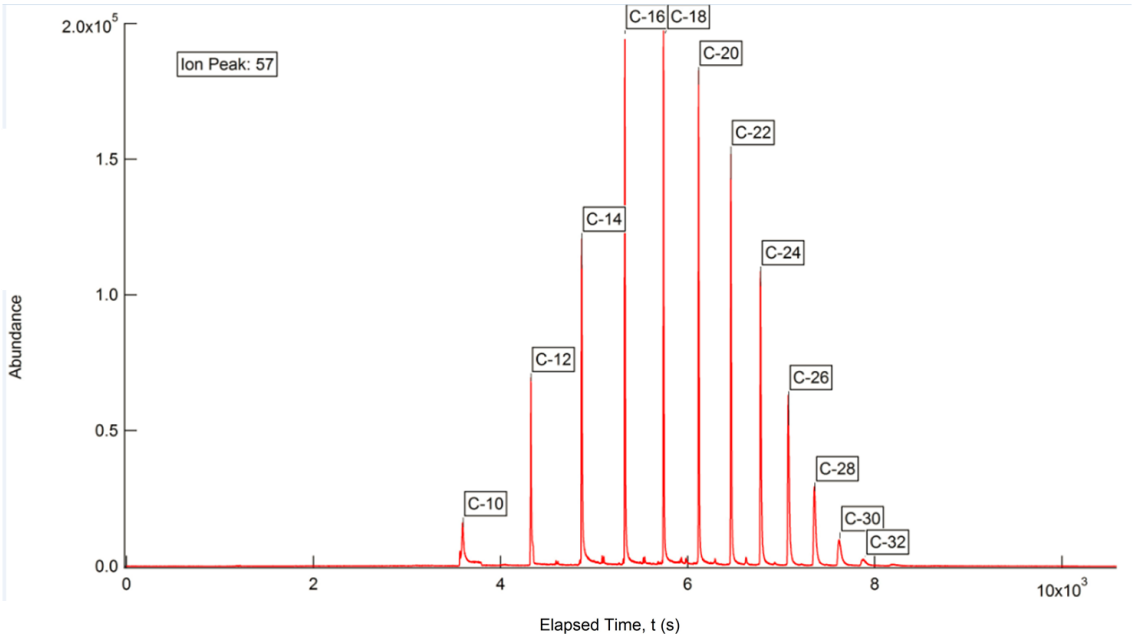

Figure 4.7 Alkane Standard Chromatogram

As can be seen, the alkanes are regularly spaced with decreasing volatility as the size of the alkane increases. The TAG GC/MS was able to measure alkanes between C10 and C32. This does not cover all of the known species injected. This means that the species are either too volatile, C8, or not volatile enough to desorb from the cell, C34-C40. Following the initial classification of the system, preliminary biomass samples are analyzed.

Previous TAG systems have been able to sample and analyze alkanes up to C40. The fact that they are not being seen here is an indication that they are sticking somewhere inside the TAG. With such large alkanes, it is crucial that all transfer components heat up to high enough temperatures. The transfer line heaters have been replaced in order to try and ensure the movement of these species. However, they were still not observed. This will become a task for future study.

Oak leaves were the first biomass source to be studied in the combustion chamber. A sample of ground leaves was placed in a stainless steel cup with a band heater. This material would burn fairly rapidly once the heater was started, about 5 minutes. The PAM chamber was set to half power for the oxidized sample. Particles were filtered (Teflon filter) and gas-phase emissions were sampled both with and without the PAM UV lamps on, and analyzed by the TAG system. The TAG was set to sample 30 minutes of every hour. First a blank is sampled to develop a background measurement. While the blank underwent

analysis, the first combustion sample is collected. After the final sample, an additional blank is analyzed in order to ensure that the cell does not have residue from the study in future measurements. The TAG collects the non-volatile particulates and semi-volatile condensable gases.

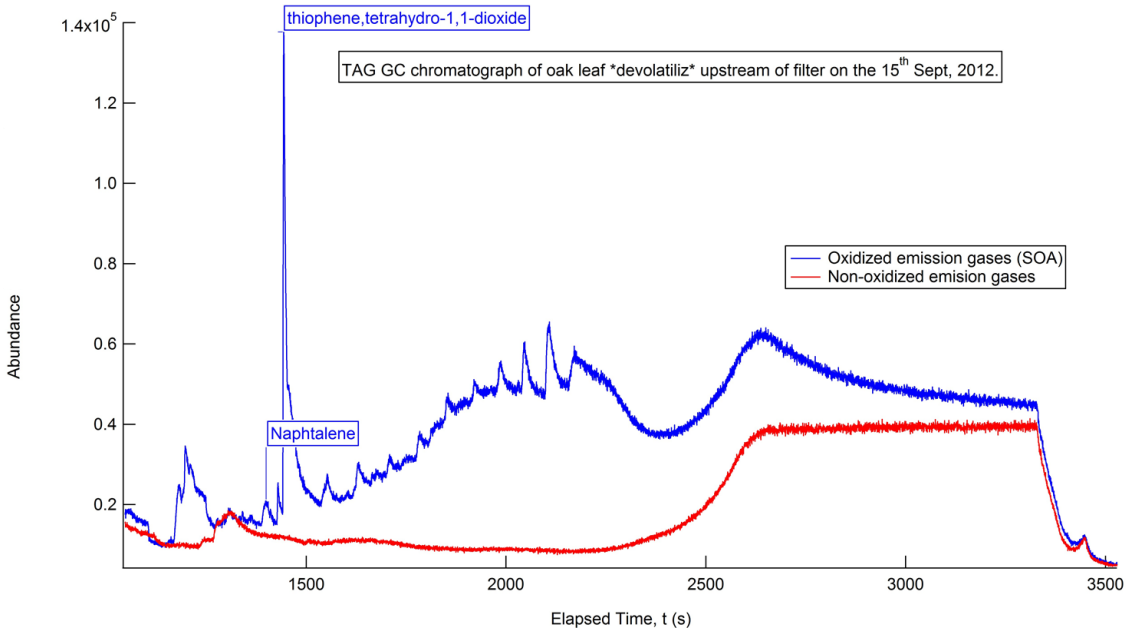

Figure 4.8 Oak Leaf Combustion – PAM oxidation – TAG Chromatogram

A)

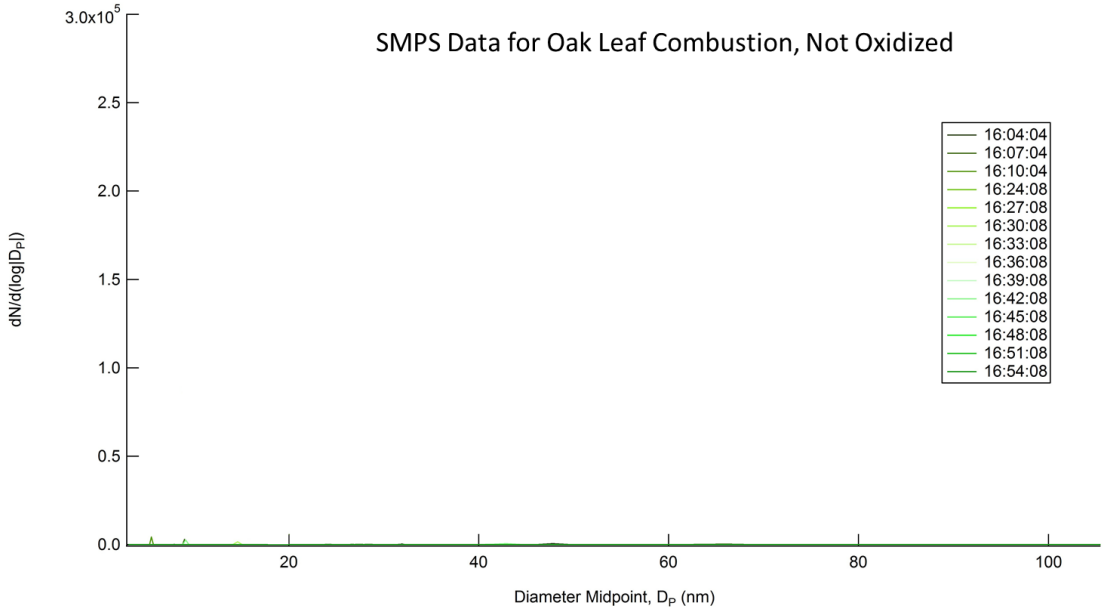

B)

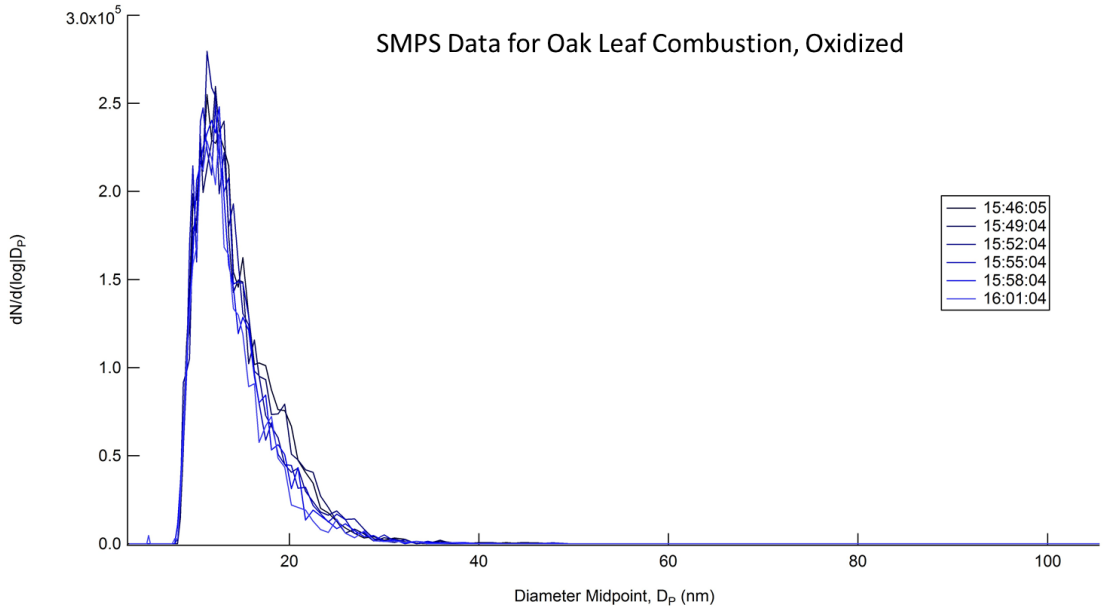

Figure 4.9 Oak Leaf Combustion SMPS Data

The non-oxidized sample does not show a large particle signal in either the chemical (TAG) or physical (SMPS) data. This is expected due to the removal of any particulate matter prior to the PAM chamber by the filter. With the UV lamps in the off position, no O_3

or OH will be produced. Therefore, no aging will be experienced by the sample. With the lamps on, particles are generated with a peak around 15nm in diameter, as shown in the SMPS data. The TAG signal also shows a much larger signal in the oxidized sample. With particles to impact and additional semi-volatile gasses to collect, the chromatogram has some resolved compounds and a large unresolved complex mixture (UCM).

The oak-leaf SOA chromatogram found here can now enter a database for single source chemical profiles. Following the initial combustion of the oak leaf, additional burns with the lamps at varying voltages will show the SOA formation and transformation process. Variable oxidation states will create an additional dimension in analysis (age-specific SOA chemical profiles for oak leaf combustion), as the obtained chromatogram will evolve as the oxidation states change.

Chapter 5

Future Work

With the system construction now completed, focus for following Combustion Chamber/PAM Chamber/TAG studies will need to be on quantification. The even alkane standard is only one form of quantification that needs to be done. There are a number of other standard injections that need to be made for the TAG in order to fully understand the ability of our TAG system to measure a wide range of species.

The extent of oxidation in the PAM chamber will be quantified. This means that the amount of O3 and OH needs to be measured. With the recent arrival of our SO_2 and O_3 gas monitors, these values can be measured. This is critical, because without these measurements, it is impossible to know the exact equivalent atmospheric aging time. The system residence times and the concentrations of OH and O_3 allow this calculation to be made. With these values and equivalent oxidation times, it is possible to start calibrating the system with the α-pinene. Due to the lack of equivalent aging times, the current α-pinene data is difficult to place in comparison to other experiments. Additional improvements to the PAM reaction chamber will include a cold junction compensation (CJC) for thermocouple reference, and better evacuation procedures for the PAM and combustion chambers for cleanout.

Following the equivalent aging times being charted for the various lamp voltages and flow rates, and verification of the chamber using α-pinene, the PAM chamber will be used to develop a library of sample profiles. Utilizing the combination of combustion chamber, PAM, and TAG, it is possible to repeatably and rapidly generate POA and SOA from a large number of sources. Pure precursor VOCs can be directly introduced to the PAM chamber, organic matter can be burned or volatilized in the combustion chamber, and combinations of the above are also possible. With this flexibility, it is possible to replicate real world emissions, and even begin to test our current analysis techniques (e.g., PMF) on known source signatures. Using our improved database of POA and SOA chemical source profiles,

PMF factors from ambient data can be better described, allowing improved source apportionment studies.

Sending these materials through the PAM chamber allows a series of profiles to be created. This achievement is where the systems' capabilities are displayed. In addition to the primary emissions (POA) being measured, various ages of SOA are measured as well, allowing for a series of age-specific chemical profiles. With new chemical profiles, it will become much easier to identify primary and secondary sources in the atmosphere. Ambient PMF factors will be matched to lab-generated profiles, allowing for better source apportionment.

An additional study that can be undertaken would be looking at the effects of organic gasses on an SMPS. Due to the SMPS being calibrated for clean air, the addition of these complex gasses could interfere with the size classifying of the SMPS since all species entering the SMPS are ionized. The addition of the ionized organic gasses could alter the charge distribution expected in the SMPS calculations. In order to see this effect, standard particles such as polystyrene latex (PSL), at different sizes, will be sent to the SMPS with and without organic gases present. Any existing POA will be filtered before the addition of the PSL particles. Looking at the difference in the measured sizes will show the interference created by the organic gases.

Appendix A

α-Pinene Oxidation Pathway, Capouet 2004

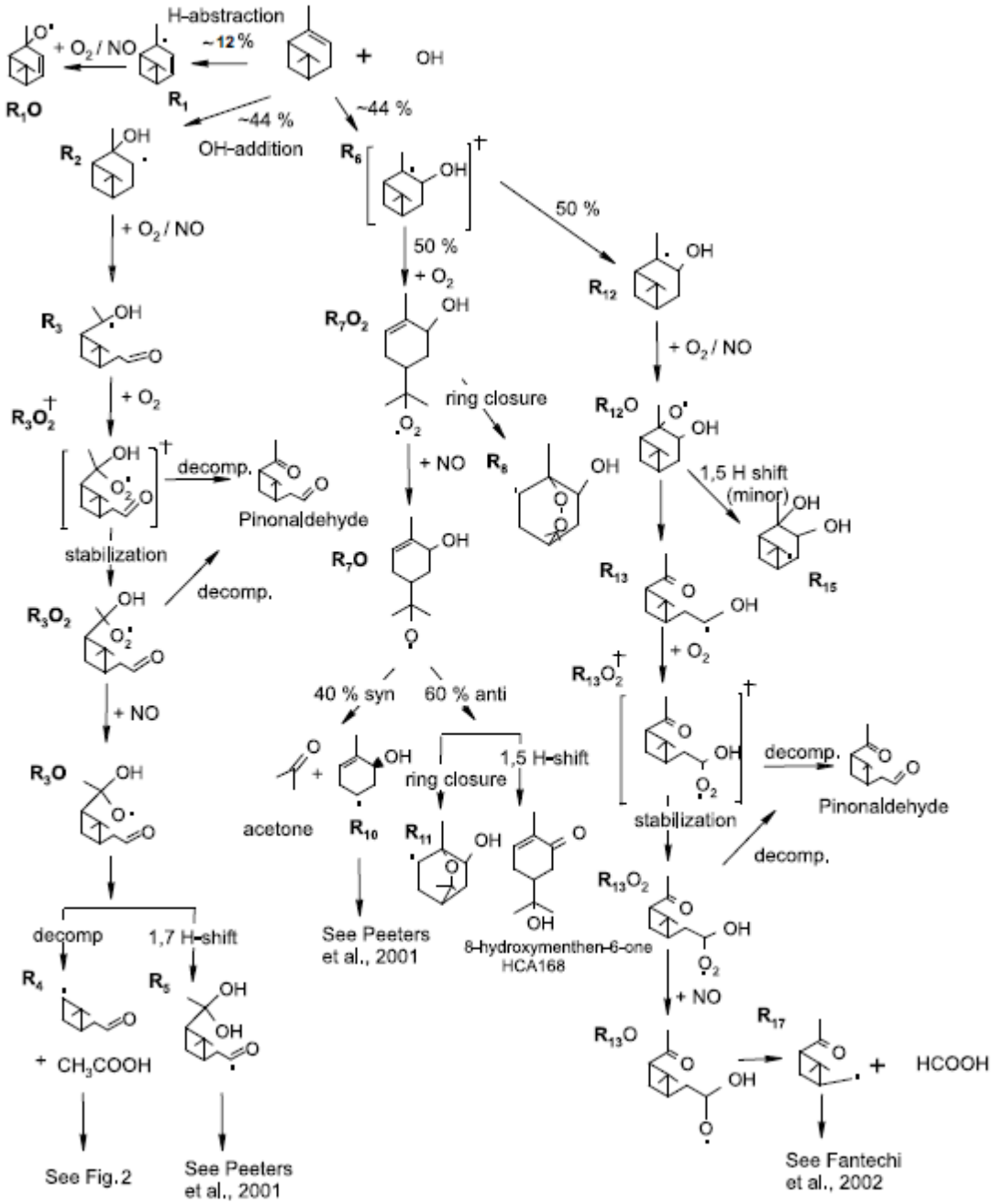

Appendix B

α-Pinene Reaction Parameters, Noziere 1999

Acetone yield

$$\alpha \times (1 - \beta) = 0.066$$

Formaldehyde yield

$$\alpha \times \beta \times \gamma \times (1 - \varepsilon) =) = 0.168$$

Overall nitrate yield

$$\alpha \times \beta \times (1 - \gamma) + (1 - \alpha) \times (1 - \delta) = 0.131$$

Pinonaldehyde yield

$$\alpha \times \beta \times \gamma \times \varepsilon + (1 - \alpha) \times \delta = 0.635$$

Appendix C

Modbus and Error Check Calculations

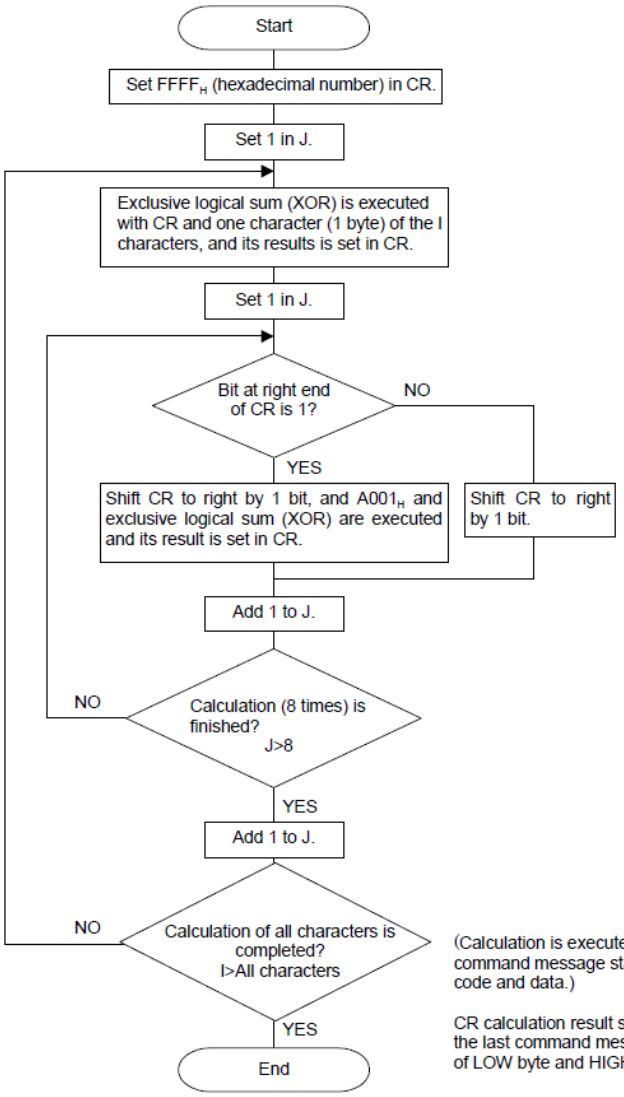

Explanation of variables
CR: CRC error check data (2 bytes)
I: Digits of calculation characters in command message
J: Check on the number of times of CR calculation

(Calculation is executed in the order of command message station No., function code and data.)

CR calculation result shall be added to the last command message in the order of LOW byte and HIGH byte.

Fig. 5-3 Flow of CRC-16 calculation

Appendix D

TAG Controls Back Panel

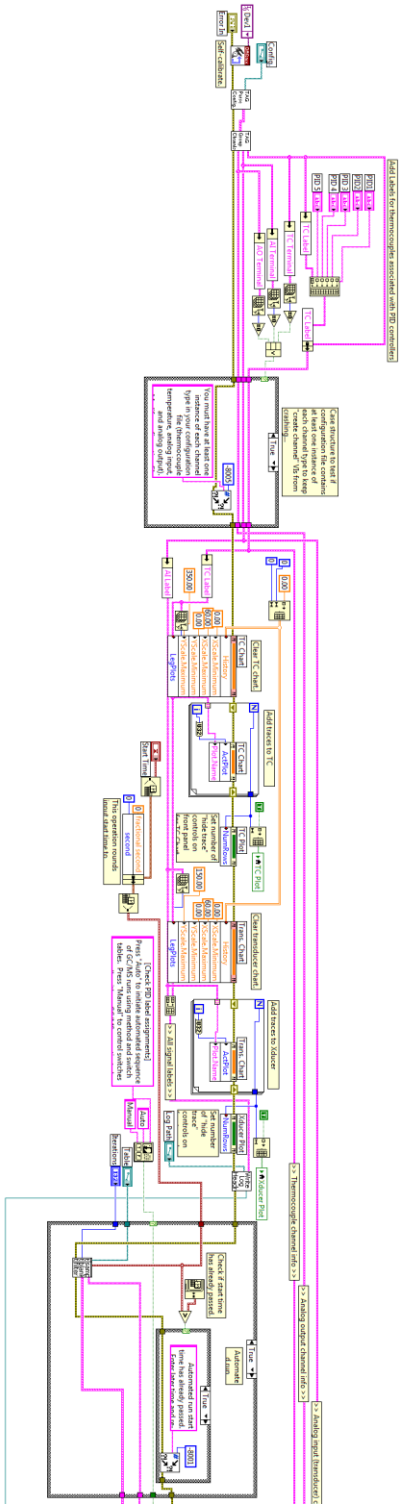

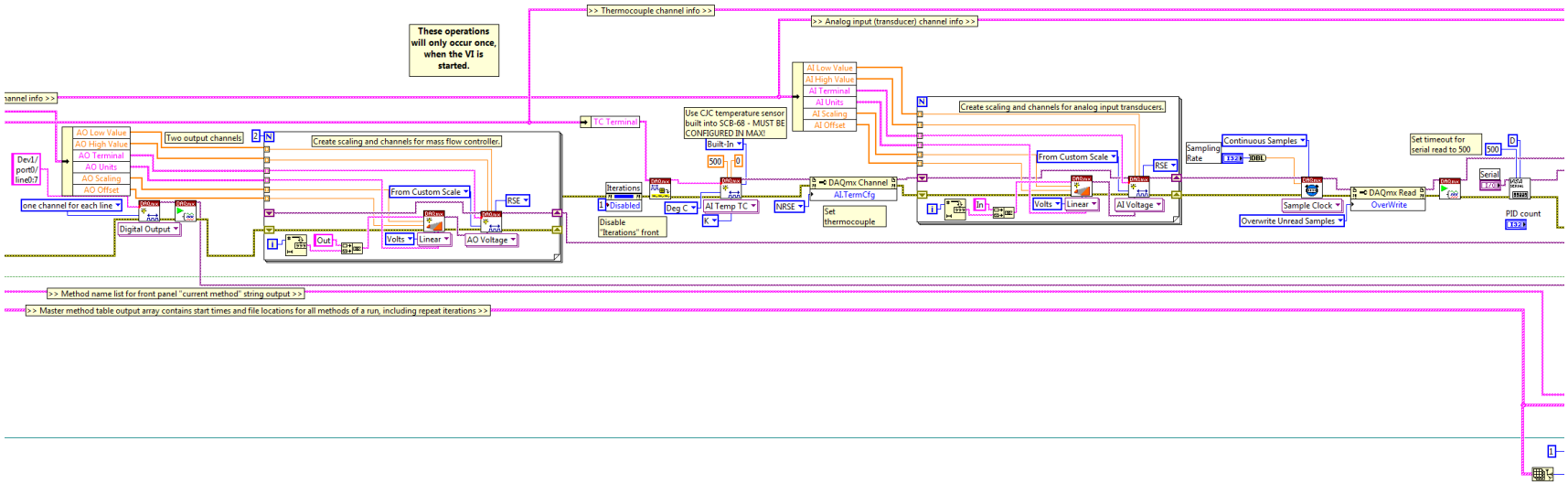
These operations will only occur once, when the VI is started.
>> Thermocouple channel info >>
>> Analog input (transducer) channel info >>
AO Low Value
AO High Value
AO Terminal
AO Units
AO Scaling
AO Offset
Two output channels
Create scaling and channels for mass flow controller.
From Custom Scale
RSE
Volts
Linear
AO Voltage
Digital Output
one channel for each line
Dev1/port0/line0:7
TC Terminal
Iterations
Disabled
Disable "Iterations" front
Use CJC temperature sensor built into SCB-68 - MUST BE CONFIGURED IN MAX!
Built-In
Deg C
K
AI Temp TC
NRSE
DAQmx Channel
AI.TermCfg
Set thermocouple
AI Low Value
AI High Value
AI Terminal
AI Units
AI Scaling
AI Offset
Create scaling and channels for analog input transducers.
AI Voltage
Sampling Rate
Continuous Samples
Sample Clock
Overwrite Unread Samples
DAQmx Read
OverWrite
Set timeout for serial read to 500
Serial
PID count
>> Method name list for front panel "current method" string output >>
>> Master method table output array contains start times and file locations for all methods of a run, including repeat iterations >>

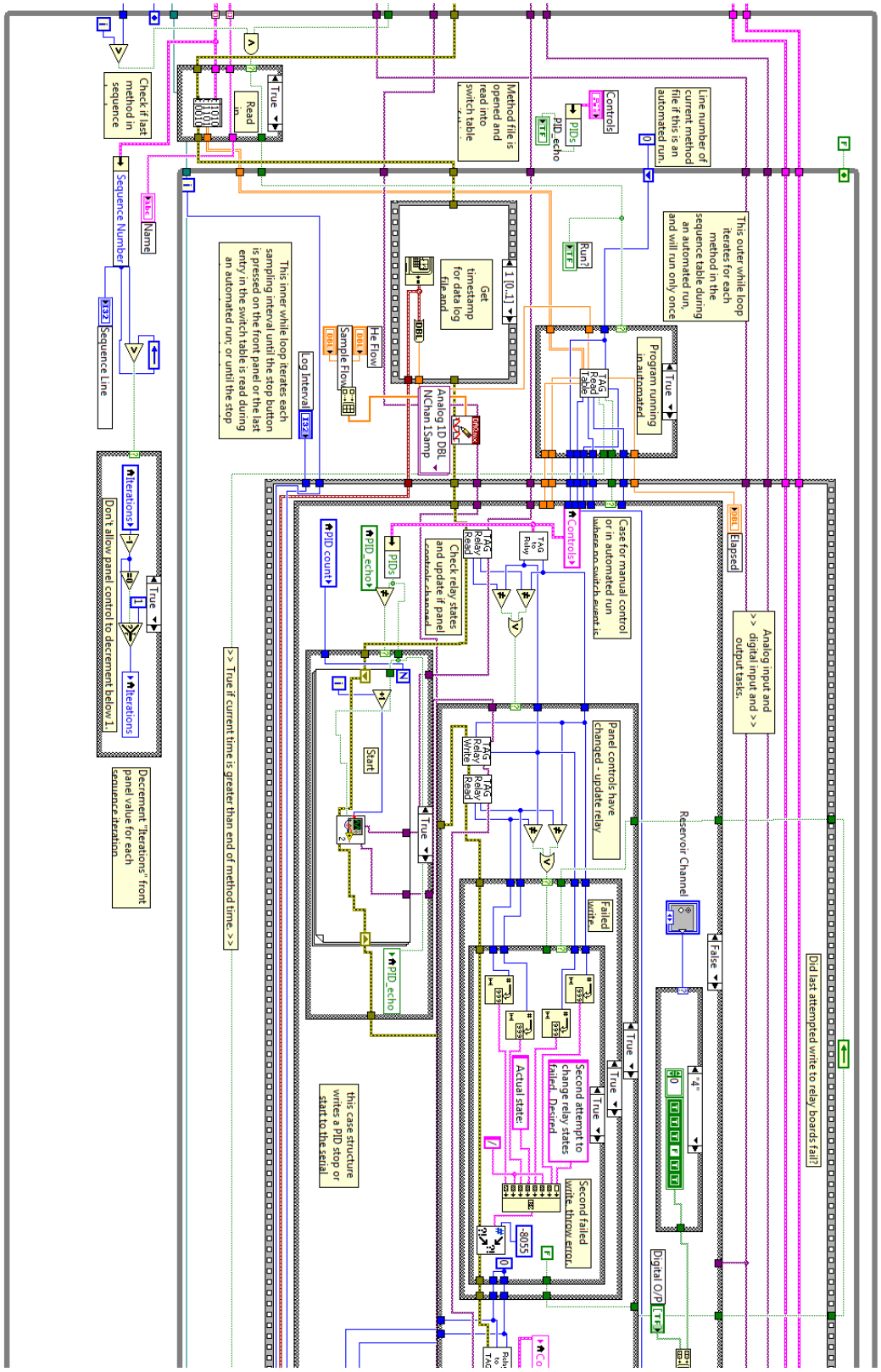
Check if last method in sequence
Read in
Method file is opened and read into switch table
Controls
PIDs
PID_echo
Line number of current method file if this is an automated run.
This outer while loop iterates for each method in the sequence table during an automated run, and will run only once
Run?
Get timestamp for data log file and
Program running in automated
Sequence Number
Name
Sequence Line
This inner while loop iterates each sampling interval until the stop button is pressed on the front panel or the last entry in the switch table is read during an automated run; or until the stop
Log Interval
He Flow
Sample Flow
Analog 1D DBL NChan 1Samp
Case for manual control or in automated run where no switch event is
Check relay states and update if panel control changed
PID_count
Start
Panel controls have changed - update relay
Analog input and >> digital input and >> output tasks.
Elapsed
Did last attempted write to relay boards fail?
Reservoir Channel
Failed write
Actual state
Second attempt to change relay states Failed_Desired
Second failed write throw error.
-8055
Digital O/P
Iterations
Don't allow panel control to decrement below 1.
Decrement "Iterations" front panel value for each sequence iteration
>> True if current time is greater than end of method time. >>
this case structure writes a PID stop or start to the serial

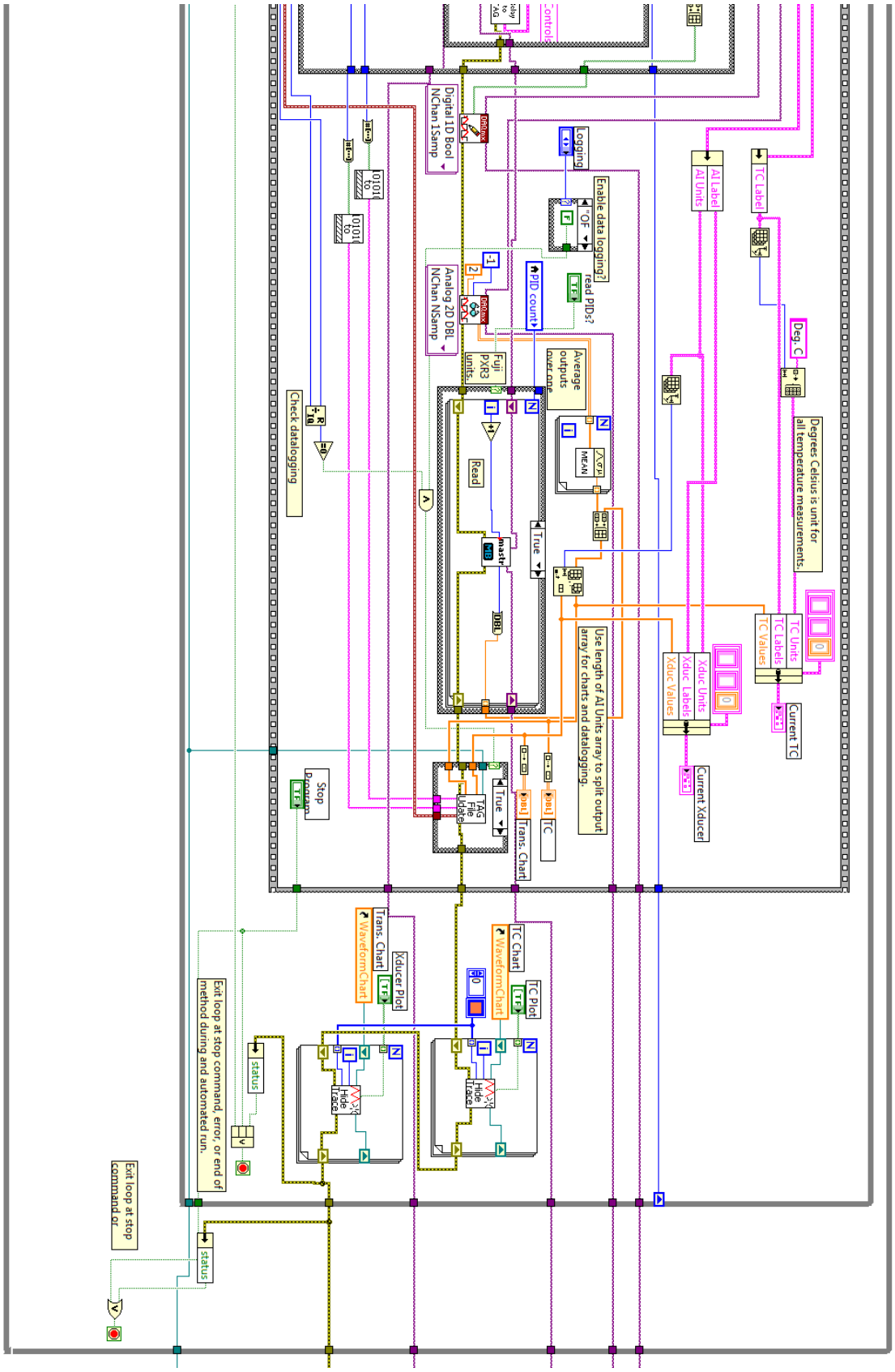
Digital 1D Bool NChan 1Samp
Logging
Enable data logging?
TF
Analog 2D DBL NChan NSamp
PID count
read PIDs?
Fuji PXR3 units
Average outputs over one
Check datalogging
Read
MEAN
True
DBL
Stop
TAS File Update
Trans. Chart
TC
Use length of AI Units array to split output array for charts and datalogging.
AI Label
AI Units
TC Label
Deg_C
Degrees Celsius is unit for all temperature measurements.
TC Values
TC Labels
TC Units
Current TC
Xduc Values
Xduc Labels
Xduc Units
Current Xducer
Trans. Chart
WaveformChart
Xducer Plot
TC Chart
TC Plot
Hide Trace
status
Exit loop at stop command or
Exit loop at stop command, error, or end of method during and automated run.

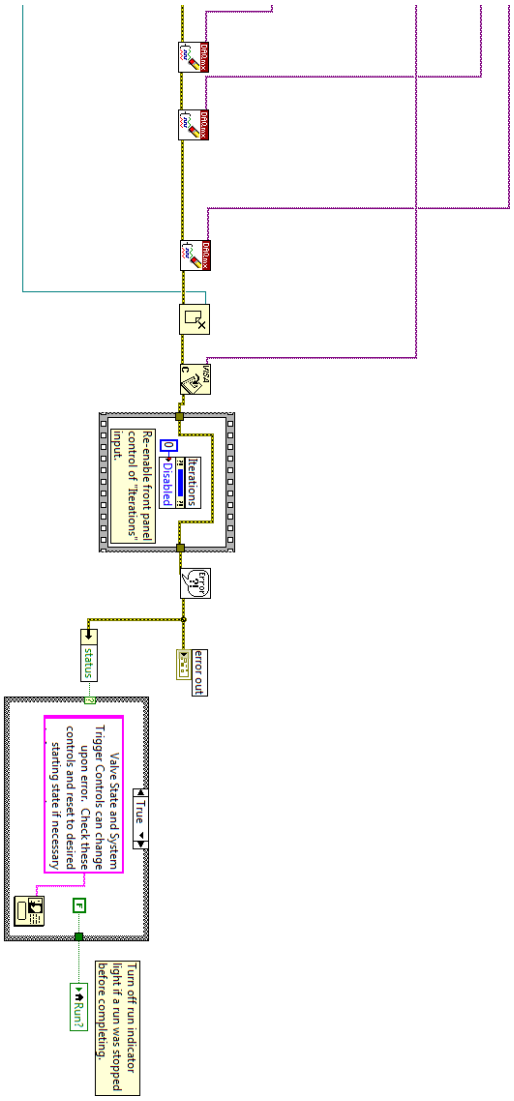
Re-enable front panel control of 'Iterations' input.
Disabled
Iterations
error out
status
Valve State and System Trigger Controls can change upon error. Check these controls and reset to desired starting state if necessary
True
Run?
Turn off run indicator light if a run was stopped before completing.

Appendix E

Cleaning Protocols

TAG

There are 2 main metrics for determining the state of the TAG system.

If the flowrate into the cell drops to 8 lpm or lower, instead of 9lpm, a jet is most likely clogged.

If a blank sample shows contamination, somewhere in the system, there is most likely residue.

In the first case,

Disassemble the collection cell.

Solvent rinse both the collection cell and the jets followed by a DI water rinse

Sonicate the jets

Bake the cell at 310 C for 1 hour.

Test flows and sample for contaminants

If there are Contaminants, the second case,

Start by identifying the location of the contamination

First run a column blank

This looks for contamination in the column.

If no contamination here, run a cell blank. This will see contamination from the column and cell so the column is checked first.

Finally, send zero air into the sample inlet to look for contaminants in the sampling lines.

If it is not possible to clean the location, it may be necessary to replace a component.

Bake the system for 1 hour at 310 C and sample again to see if the contaminants have been removed.

PAM

Passing Zero Air through the PAM chamber should result in no particulates, even if the lamps are on.

If particulates appear, the system needs to be cleaned

Turn on the lamps to full voltage and have O2 and pure air flowing through.

Leave on overnight.

If there are still particulates, disassemble the system and clean the inside with a solvent rinse

After a sampling campaign or especially dirty sample, the inside of the PAM chamber should be cleaned in order to ensure no future contaminants.

Occasionally, if other cleaning methods are not working, the inner walls of the PAM chamber may need to be solvent rinsed.

Combustion Chamber

Use the same metrics as the PAM to determine if there is off-gassing in the chamber.

Comparing a PAM-oxidized combustion chamber background to PAM-oxidized ultra-pure air, we can see how much internal contamination there is from the combustion chamber.

Frequency: Between major experiments and when the chamber off gasses,

If contaminated, solvent rinse the interior of the two chamber portions.

Can also try to send hot air, ~40C, into the chamber in order to volatilize semi volatiles that are off-gassing.

Appendix F

Operating Protocols

COMBUSTION CHAMBER: STANDARD OPERATING PROTOCOL

Saftey: Lab gloves should be on at all times of operation. When not in use, the doors should be secured shut and any heating unit off.

Setting Up:

1. Unlock the doors of the combustion chamber.

2. Check that the chamber is clean (no ash or residue visible). Clean if residue is present.

3. Check for contaminants by measuring a blank sample with zero air. If contaminated follow cleaning protocol

4. Control the flowrates of (i) vacuum and (ii) particle/gas-free air to the chamber.

   this can be done by ball valves and needle valves in the air lines

5. Remove the plug between the combustion chamber and mixing chamber.

6. Place biomass of choice in cup holder or cup holders.

7. Ensure online instruments / downstream network is set up and ready to run.

Running the System:

7. If burning with butane igniter first ignite, then close the doors, securing them with the latches.

8. If volatilizing/combusting with heating mantle first close the doors. The heater is controlled by an outlet.

Venting and Shutdown:

Safety: at the end of experiment you must (i) ensure there is no flame or smoke or ember in any biomass sample and (ii) heating mantle is unplugged.

9. After all data desired is collected, don't open the doors immediately.

Safety: don't open the doors after a burn until one hour after venting.

10. The system can be vented by opening the valves on the vacuum and particle/gas-free air.

11. After the system vented for an hour, remove the cup from the heating mantle / platform.

12. Close the doors securing them with the latches and keep venting until next experiments.

P.A.M. REACTOR: STANDARD OPERATING PROTOCOL

1. Check the background levels of the PAM chamber and clean if necessary, following the provided protocol.

2. Ensure the valves are in the desired position for flow of the sample.

3. Open the valve of the N2 tank. The flow is controlled by the MFC / orifice.

4. Open the valve of the O2 tank. The flow is controlled by the MFC / orifice.

Safety: Ensure the vent after the denuder is directed towards the hood. If sampling particles from the combustion chamber, close the vent. If you regulate any flowrates yourself, then make sure there is no pressure buildup – that is what the vent is for.

5. Turn on the variable voltages to a desired voltage for the UV lamps (2 in PAM and 1 for O3).

6. The reactor is ready to be connected to a physical or chemical detection instrument.

T.A.G. SYSTEM: STANDARD OPERATING PROTOCOL

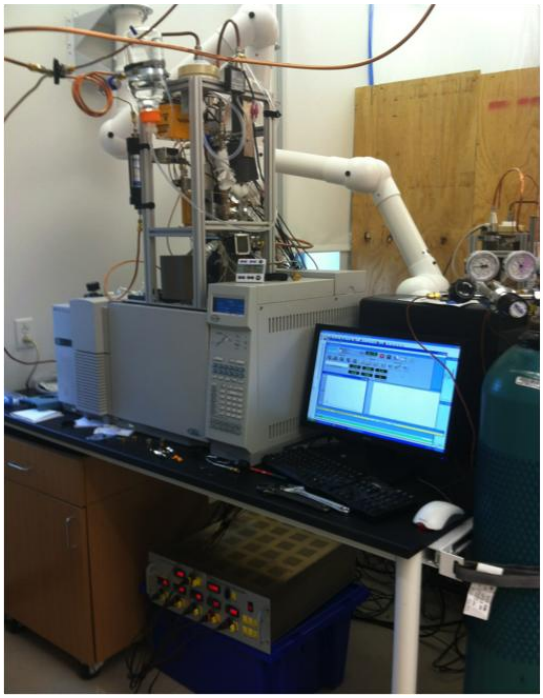

1. Following the cleaning protocol, check to ensure that the system is clean.

2. Check the vacuum to the TAG is open and pulling properly.

3. Check that the He line is in the open position.

4. Verify the temperatures for the 6-port valve and transfer line are at 300 C. If they are not, do not operate the valve.

Safety: Check the temperatures on all components before working with them. Many components are maintained at high temperatures.

5. In the Labview control program, load the correct sequence table.

6. In Chemstation, modify the sequence in order to match the desired sampling sequence.

7. Run Sequence in Chemstation.

8. In Labview, set the automatic start time to any time after the current time.

9. Start Labview, select automatic run.

10. The system will automatically collect and analyze the sample.

References

[1] Trenberth, K.E., P.D. Jones, P. Ambenje, R. Bojariu, D. Easterling, A. Klein Tank, D. Parker, F. Rahimzadeh, J.A. Renwick, M. Rusticucci, B. Soden and P. Zhai, 2007: Observations: Surface and Atmospheric Climate Change. Climate Change 2007: The Physical Science Basis. Contribution of Working Group I to the Fourth Assessment Report of the Intergovernmental Panel on Climate Change [Solomon, S., D. Qin, M. Manning, Z. Chen, M. Marquis, K.B. Averyt, M. Tignor and H.L. Miller (eds.)]. Cambridge University Press, Cambridge, United Kingdom and New York, NY, USA.

[2] Q. Zhang, J. L. Jimenez, M. R. Canagaratna, J. D. Allan, H. Coe, I. Ulbrich, M. R. Alfarra, A. Takami, A. M. Middlebrook, Y. L. Sun, K. Dzepina, E. Dunlea, K. Docherty, P. F. DeCarlo, D. Salcedo, T. Onasch, J. T. Jayne, T. Miyoshi, A. Shimono, S. Hatakeyama, N. Takegawa, Y. Kondo, J. Schneider, F. Drewnick, S. Borrmann, S. Weimer, K. Demerjian, P. Williams, K. Bower, R. Bahreini, L. Cottrell, R. J. Griffin, J. Rautiainen, J. Y. Sun, Y. M. Zhang, D. R. Worsnop. Ubiquity and dominance of oxygenated species in organic aerosols in anthropogenically-influenced Northern Hemisphere midlatitudes, Geophys. Res. Lett., 34, L13801, doi:10.1029/2007GL029979, 2007b.

[3] Hao, L. Q., Romakkaniemi, S., Yli-Pirilä, P., Joutsensaari, J., Kortelainen, A., Kroll, J. H., Miettinen, P., Vaattovaara, P., Tiitta, P., Jaatinen, A., Kajos, M. K., Holopainen, J. K., Heijari, J., Rinne, J., Kulmala, M., Worsnop, D. R., Smith, J. N., and Laaksonen, A.: Mass yields of secondary organic aerosols from the oxidation of α-pinene and real plant emissions, Atmos. Chem. Phys., 11, 1367-1378, doi:10.5194/acp-11-1367-2011, 2011.

[4] Kang, E., Toohey, D. W., and Brune, W. H.: Dependence of SOA oxidation on organic aerosol mass concentration and OH exposure: experimental PAM chamber studies, Atmos. Chem. Phys. Discuss., 10, 24053-24089, doi:10.5194/acpd-10-24053-2010, 2010.

[5] Eddingsaas, N. C., Loza, C. L., Yee, L. D., Seinfeld, J. H., and Wennberg, P. O.: α-pinene photooxidation under controlled chemical conditions – Part 1: Gas-phase composition in low- and high-NO_x environments, Atmos. Chem. Phys., 12, 6489-6504, doi:10.5194/acp-12-6489-2012, 2012

[6] Kroll, J. H., Donahue, N. M., Jimenez, J. L., Kessler, S. H., Canagaratna, M. R., Wilson, K. R., Altieri, K. E., Mazzoleni, L. R., Wozniak, A. S., Bluhm, H., Mysak, E. R., Smith, J. D., Kolb, C. E., and Worsnop, D. R.: Carbon oxidation state as a metric for describing the chemistry of atmospheric organic aerosol, Nat. Chem., 3, 133–139, doi:110.1038/NCHEM.1948, 2011.

[7] Aumont, B., Szopa, S., and Madronich, S.: Modelling the evolution of organic carbon during its gas-phase tropospheric oxidation: development of an explicit model based on a self generating approach, Atmos. Chem. Phys., 5, 2497–2517, doi:10.5194/acp-5-2497-2005, 2005.

[8] Valorso, R., Aumont, B., Camredon, M., Raventos-Duran, T., Mouchel-Vallon, C., Ng, N. L., Seinfeld, J. H., Lee-Taylor, J., and Madronich, S.: Explicit modelling of SOA formation from α-pinene photooxidation: sensitivity to vapour pressure estimation, Atmos. Chem. Phys., 11, 6895-6910, doi:10.5194/acp-11-6895-2011, 2011.

[9] Capouet, M., Peeters, J., Nozi`ere, B., and Müller, J.-F.: Alpha-pinene oxidation by OH: simulations of laboratory experiments, Atmos. Chem. Phys., 4, 2285-2311, doi:10.5194/acp-4-2285-2004, 2004.

[10] Nozière, B., I. Barnes, and K.-H. Becker (1999), Product study and mechanisms of the reactions of α-pinene and of pinonaldehyde with OH radicals, *J. Geophys. Res.*,*104*(D19), 23,645–23,656, doi:10.1029/1999JD900778.

[12] Pathak, R. K., C. O. Stanier, N. M. Donahue, and S. N. Pandis (2007), Ozonolysis of a-pinene at atmospherically relevant concentrations: Temperature dependence of aerosol mass fractions (yields), J. Geophys. Res., 112, D03201, doi:10.1029/2006JD007436.

[13] Hao, L. Q., Romakkaniemi, S., Yli-Pirilä, P., Joutsensaari, J., Kortelainen, A., Kroll, J. H., Miettinen, P., Vaattovaara, P., Tiitta, P., Jaatinen, A., Kajos, M. K., Holopainen, J. K., Heijari, J., Rinne, J., Kulmala, M., Worsnop, D. R., Smith, J. N., and Laaksonen, A.: Mass yields of secondary organic aerosols from the oxidation of α-pinene and real plant emissions, Atmos. Chem. Phys., 11, 1367-1378, doi:10.5194/acp-11-1367-2011, 2011.

[14] Lambe, A. T., Ahern, A. T., Williams, L. R., Slowik, J. G., Wong, J. P. S., Abbatt, J. P. D., Brune, W. H., Ng, N. L., Croasdale, D. R., Wright, J. P., Worsnop, D. R., Davidovits, P., and Onasch, T. B.: Characterization of aerosol photooxidation flow reactors: heterogeneous oxidation, secondary organic aerosol formation and cloud condensation nuclei activity measurements, Atmos. Meas. Tech. Discuss., 3, 5211-5251, doi:10.5194/amtd-3-5211-2010, 2010.

[15] Kang, E., Toohey, D. W., and Brune, W. H.: Dependence of SOA oxidation on organic aerosol mass concentration and OH exposure: experimental PAM chamber studies, Atmos. Chem. Phys., 11, 1837-1852, doi:10.5194/acp-11-1837-2011, 2011.

[16] Kang, E., Root, M. J., Toohey, D. W., and Brune, W. H.: Introducing the concept of Potential Aerosol Mass (PAM), Atmos. Chem. Phys., 7, 5727-5744, doi:10.5194/acp-7-5727-2007, 2007.

[17] Lambe, A. T., Onasch, T. B., Massoli, P., Croasdale, D. R., Wright, J. P., Ahern, A. T., Williams, L. R., Worsnop, D. R., Brune, W. H., and Davidovits, P.: Laboratory studies of the chemical composition and cloud condensation nuclei (CCN) activity of secondary organic aerosol (SOA) and oxidized primary organic aerosol (OPOA), Atmos. Chem. Phys., 11, 8913-8928, doi:10.5194/acp-11-8913-2011, 2011.

[18] Spracklen, D. V., Carslaw, K. S., Pöschl, U., Rap, A., and Forster, P. M.: Global cloud condensation nuclei influenced by carbonaceous combustion aerosol, Atmos. Chem. Phys., 11, 9067-9087, doi:10.5194/acp-11-9067-2011, 2011.

[19] Williams, B.J., Goldstein, A.H., Kreisberg, N.M., and Hering, S.V., An in-situ instrumentfor speciated organic composition of atmospheric aerosols: Thermal Desorption Aerosol GC/MS-FID (TAG), Aerosol Science & Technology, 40, 627-638, 2006.

[21] Wolfgang F. Rogge , Lynn M. Hildemann , Monica A. Mazurek , Glen R. Cass , Bernd R. T. Simoneit. Sources of fine organic aerosol. 3. Road dust, tire debris, and organometallic brake lining dust: roads as sources and sinks, Environmental Science & Technology, 27,1892-1904, 1993

[22] Wolfgang F. Rogge , Lynn M. Hildemann , Monica A. Mazurek , Glen R. Cass , Bernd R. T. Simoneit. Sources of Fine Organic Aerosol. 7.Hot Asphalt Roofing Tar Pot Fumes, Environmental Science & Technology, 31,2726-2730, 1997

[23] Wolfgang F. Rogge , Lynn M. Hildemann , Monica A. Mazurek , Glen R. Cass , Bernd R. T. Simoneit. Sources of Fine Organic Aerosol. 9. Pine, Oak, and Synthetic Log Combustion in Residential Fireplaces, Environmental Science & Technology, 32, 13-22, 1998

[24] Jimenez, J.L., et al, Evolution of Organic Aerosols in the Atmosphere, Science, 326, 1525-1529, 2009.

[25] Jayne, J.T., Leard, D.C., Zhang, X., Davidovits, P., Smith, K.A., Kolb, C.E., and Worsnop, D.R., Development of an Aerosol Mass Spectrometer for Size and Composition Analysis of Submicron Particles, Aerosol Science and Technology, 33, 49-70, 2000.

[26] DeCarlo, P.F., Jimenez, J.L., et al, Field-Deployable, High-Resolution, Time-of-Flight Aerosol Mass Spectrometer, Analytical Chemistry, 78, 8281-8289, 2006.

[27] Sioutas, C.; Abt, E.; Wolfson, J.M.; Koutrakis, P. Evaluation of the measurement performance of the scanning mobility particle sizer and aerodynamic particle sizer. Aerosol Sci. Technol.1999, 30, 84–92

[29] Fuji Electric Systems Co., Ltd. MICRO CONTROLLER X COMMUNICATION FUNCTIONS (RS-485 Z-ASCII)

[30] Fuji Electric Systems Co., Ltd. MICRO CONTROLLER X COMMUNICATION FUNCTIONS (RS-485 MODBUS)

[31] Griffin, R.J., Cocker, D.R III, Flagan, R.C., Seinfeld, J.H. Organic Aerosol Formation from the Oxidatino of Biogenic Hydrocarbons, Journal of Geophysical Research, 104, D3, 3555-3567, 1999

[32] Ulbrich, I.M., Canagaratna, M.R., Zhang, Q., Worsnop, D.R., and Jimenez., J.L. Interpretation of Organic Components from Positive Matrix Factorization of Aerosol Mass Spectrometric Data. *Atmospheric Chemistry and Physics* , 9(9), 2891-2918, 2009

[33] Zhong, J. PID Controller Tuning: A Short Tutorial. Purdue University, 2006

[33] Isaacman, G., Kreisberg, N. M., Worton, D. R., Hering, S. V., and Goldstein, A. H.: A versatile and reproducible automatic injection system for liquid standard introduction: application to in-situ calibration, Atmos. Meas. Tech., 4, 1937-1942, doi:10.5194/amt-4-1937-2011, 2011.

Vita

Peter Johnson Mellott

Degrees	B.S. with Honors, Chemical Engineering, May 2010
Professional Societies	Tau Beta Pi American Institute of Chemical Engineering

December 2012